PB 181511
Price $1.00

A STUDY OF BRITTLE FRACTURE INITIATION IN MILD STEEL

SSC-147

BY

F. W. BARTON AND W. J. HALL

SHIP STRUCTURE COMMITTEE

For sale by the U. S. Department of Commerce, Office of Technical Services,
Washington, D.C. 20230

SHIP STRUCTURE COMMITTEE

MEMBER AGENCIES:

BUREAU OF SHIPS, DEPT. OF NAVY
MILITARY SEA TRANSPORTATION SERVICE, DEPT. OF NAVY
UNITED STATES COAST GUARD, TREASURY DEPT.
MARITIME ADMINISTRATION, DEPT. OF COMMERCE
AMERICAN BUREAU OF SHIPPING

ADDRESS CORRESPONDENCE TO:

SECRETARY
SHIP STRUCTURE COMMITTEE
U. S. COAST GUARD HEADQUARTERS
WASHINGTON 25, D. C.

15 July 1963

Dear Sir

As part of its research program directed toward the improvement of hull structures of ships, the Ship Structure Committee has been sponsoring a brittle-fracture mechanics study at the University of Illinois.

Herewith is a technical report, SSC-147, A Study of Brittle Fracture Initiation in Mild Steel, by F. W. Barton and W. J. Hall.

This project was conducted under the advisory guidance of the Committee on Ship Structural Design of the National Academy of Sciences-National Research Council.

This report is being distributed to the individuals and agencies associated with the project, and to those interested in the Ship Structure Committee program. Questions or comments regarding this report would be appreciated and should be sent to the Secretary, Ship Structure Committee.

Sincerely yours,

T. J. Fabik
Rear Admiral, U. S. Coast Guard
Chairman, Ship Structure Committee

Serial No. SSC-147

Technical Report

on

Project SR-155

to the

SHIP STRUCTURE COMMITTEE

on

A STUDY OF BRITTLE FRACTURE INITIATION IN MILD STEEL

by

F. W Barton and W. J. Hall
Department of Civil Engineering
University of Illinois

under

Bureau of Ships
Department of the Navy
Contract NObs-65790

transmitted through

Committee on Ship Structural Design
Division of Engineering and Industrial Research
National Academy of Sciences-National Research Council

under

Department of the Navy
Bureau of Ships Contract NObs-84321

Washington, D. C.
U. S. Department of Commerce, Office of Technical Services

July 15, 1963

ABSTRACT

The purpose of this investigation was to study the conditions of brittle-fracture initiation in low-carbon steel. An elastic-plastic stress analysis was developed from which the state of stress along the minimum section of a notched specimen could be determined as a function of the average applied stress and the yield stress. A series of tests on plate-type specimens, with the same notch configuration as that used in the stress analysis, provided experimental values of average fracture stress under various test conditions.

Application of the elastic-plastic stress analysis to the experimental results provided a theoretical prediction of the state of stress at the instant and location of fracture initiation and also an indication of the position of the elastic-plastic boundary at fracture. It was found that the stress condition necessary for brittle fracture initiation, in the mild-steel specimens studied, was achieved when the maximum tensile stress reached a critical value of approximately 246,000 psi. For a ratio of average applied stress to yield stress above a certain value, the maximum tensile stress cannot attain the necessary stress value for the initiation of a brittle fracture as defined herein, and the resulting fracture will be ductile in nature, preceded by gross plastic deformation.

Results from this investigation were compared with existing information related to fracture initiation to provide a basis for evaluating both the analytical technique employed and the final results obtained.

CONTENTS

SR-155 PROJECT ADVISORY COMMITTEE

"Low-Velocity Fracture"

for the

COMMITTEE ON SHIP STRUCTURAL DESIGN
Division of Engineering & Industrial Research
National Academy of Sciences-National Research Council

Chairman:

Dana Young
Southwest Research Institute

Members:

J. S. Clarke
Esso Research & Engineering Company

J. M. Frankland
National Bureau of Standards

J. M. Krafft
Naval Research Laboratory

NOMENCLATURE

$2a$	Minimum section width of specimen (1 in.)
ρ	Root radius of hyperbolic notch (0.01 in.)
d	Finite-difference net spacing (a/16)
φ	Stress Function
σ_{YS}	Yield stress in simple tension corresponding to a given temperature
P	Applied Load
σ_A	Average applied stress across minimum section $(\frac{P}{2a})$
σ_{AF}	σ_A at fracture
σ_A/σ_{YS}	Stress ratio corresponding to applied load
X_P	Distance from coordinate origin to elastic-plastic boundary

INTRODUCTION

General

Fracture has been defined as the separation or fragmentation of a solid body into two or more parts under the action of stress.[1] For most structural metals and alloys this process of separation is classified into the two general categories of ductile and brittle fracture. The usual distinction between the two types of fracture is made on the basis of the amount of plastic deformation preceding actual separation. Ductile fracture is preceded by extensive plastic flow, not only during fracture initiation, but also during relatively slow fracture propagation and finally separation. This is the type of fracture most commonly observed in structural metals such as low-carbon steel. Brittle fracture, on the other hand, is characterized by a rapid rate of crack propagation with no gross plastic deformation during any stage and very little microdeformation. The predominant feature of a brittle fracture in service is that usually it is unexpected and cannot be anticipated on the basis of conventional design criteria.

To facilitate the study of brittle fracture, it is convenient to separate the total brittle-fracture process into two stages, initiation and propagation. Since the investigation reported herein was concerned with the conditions related to initiation of a brittle fracture, the propagation aspect is not discussed in this report. The study of initiation can be conducted on a microscopic level (atomic or molecular) in which the material is considered to be discontinuous and made up of discrete particles, or it can be conducted on the phenomenological (large scale) level in which the material is considered to be continuous and homogeneous and to be composed of identical volume elements of finite dimensions. The former area is the domain of metallurgists and solid state physicists. The investigation described in this report was conducted within the phenomenological realm with engineering design applications in mind.

In the phenomenological study of initiation it is necessary to consider macroscopic factors that influence the phenomenon of initiation. Of these factors, probably the most important is the general state of stress at the origin of fracture initiation, and in particular the maximum tensile stress present. A determination of a maximum critical stress, or a critical stress ratio necessary for brittle fracture initiation would certainly provide the simplest basis for improved design procedures. In order to effectively make use of a critical stress in design it would also be necessary to have available effective stress concentration factors for the more prevalent types of flaws or cracks expected in a material. From a knowledge of the maximum tensile stress required for fracture initiation, the average applied stress at which a brittle fracture would be expected to occur could easily be predicted. Regardless of practical implications, however, a knowledge of the maximum stress, and general stress state at fracture is a necessary part of a total understanding of the mechanism of brittle fracture initiation.

Related Work

Since this report is concerned with the general state of stress, and in particular the maximum normal stress, existing at the fracture origin, a summary of recent work relating

to this particular aspect of fracture initiation is presented in this section.

Jenkins and his associates[2] found that, for brittle fracture, it appears that the maximum normal stress and the ratio of maximum normal stress to maximum shearing stress are the most significant factors, and these concepts are apparently accepted by many investigators. Cottrell,[3] in discussing the fracture transition mode from ductile to brittle, expressed the view that a large ratio of maximum normal to maximum shear stress can aid materially in causing such a transition.

Davis, Parker and Boodberg[4] conducted several fracture tests on plate specimens of mild steel in a study of the shear to cleavage fracture transition. The state of stress, defined in part by the ratio of maximum tensile stress to maximum shear stress, was found to be directly related to the transition temperature. The likelihood of brittle fractures occurring at normal temperature is increased if the ratio of maximum tensile to shear stress is increased by means of a notch. Also it was concluded that brittle fractures initiate at the mid-thickness of a plate, where the tensile stress in the thickness direction is a maximum.

Weiss, Sessler and others[5-6] analyzed the notch properties of high strength sheet alloys as a function of test temperatures and initial stress distribution. In extremely brittle alloys, the stress gradient is the predominant factor influencing notch strength. Other factors, such as specimen geometry and elastic stress-concentration factors, are significant only insofar as their contribution to the magnitudes of the stress gradient and the maximum stress in the region of the notch root.

Grinter,[7] in a qualitative discussion only, reasoned that in a notched steel plate of sufficient thickness, the tensile stress in the thickness direction could attain a value at least equal to the uniaxial yield stress. He expressed the view that this tensile stress could be significant for plate thickness of 1/4 in. or more. He also qualitatively described a mechanism by which the maximum axial stress could reach a value of approximately 2.75 times the yield stress.

Yukawa and McMullin[8] tested a series of notched bar specimens in bending utilizing different sizes of specimens and different notch preparations. They found that the limiting strength, calculated from bending theory, was approximately 260,000 psi, and that for specimens less than 1 in. in size, very little variation was observed in fracture strength.

The most recent work pertaining directly to the investigation reported herein was conducted by Hendrickson, Wood, and Clark[9-10] at the California Institute of Technology. In their investigation, small notched cylindrical specimens of annealed mild steel were tested over a range of temperatures and loading rates. From the initial study of yielding, results showed that the maximum stress for local yielding in a notched specimen was the same value as the static upper yield stress in unnotched specimens. Also there was apparently no indication of delayed yielding in the notched specimens.

In a later study of the same nature, the state of stress at the minimum cross-section of a notched cylindrical specimen subjected to tensile loading was determined by means of an elastic-plastic stress analysis. An experimental study supplied values of average fracture stress for the range of conditions employed. The true maximum tensile stress at the position and at the instant of initiation of brittle fracture was determined from experimental results by the application of the stress analysis. They found that brittle fracture is initiated in their mild steel specimens when a critical maximum tensile stress of about 210,000 psi is attained. This value was found to be independent of stress rate and temperature.

The results of their investigation also indicated that a necessary condition for brittle fracture is that the ratio between the average applied stress and the yield stress never attains the critical value which would cause yielding to progress to the axis of the specimen.

Object and Scope

The purpose of this investigation was to determine the maximum tensile stress and the corresponding stress field present in a notched steel specimen at the instant of fracture. An approximate elastic-plastic stress analysis was developed as a part of the investigation. Also included as a part of the investigation was a study of the fracture behavior of notched

steel plates and a study of the effect of certain parameters on fracture behavior.

In this investigation a series of notched flat plate specimens were tested in tension at a fixed gradual rate of loading. With the exception of temperature and thickness all other test parameters were held constant. Test temperatures were varied from room temperature (78 F) down to liquid nitrogen temperature (-320 F), and nominal specimen thickness varied from 1/4 in. to 1 in. The results from the experimental study were combined with the results from the approximate elastic-plastic stress analysis developed as a part of this investigation to obtain the desired information regarding the state of stress in the specimen. This analysis makes it possible to predict the applied load at which general yielding will occur and thus provided a dividing line between brittle and ductile fracture. The analysis also provided a theoretical prediction of the position of the elastic-plastic boundary in the specimens.

The final results of this study include a theoretical prediction of the maximum tensile stress necessary for fracture initiation under the conditions studied, a description of the stress state at fracture for the particular test conditions employed, and a prediction of the ratio of average applied stress to yield stress above which only ductile fractures are possible. In addition, the results originating from this investigation are compared with related fracture studies previously conducted and the validity and applicability of the results are analyzed and discussed.

The following sections of this report contain the development of the elastic-plastic stress analysis and a discussion of the application and utilization of this analysis; a description of the experimental phase of the investigation including specimen description, test procedure and results; the analysis and discussion of the results of the study; and a summary of the program and conclusions drawn from the study.

ANALYTICAL STUDY

General

The mechanism of fracture initiation at a notch in a plate-type tensile specimen is a complex and little understood phenomenon. It is known, however, that although the stress state in the vicinity of a notch in a tensile specimen is difficult to analyze, triaxial tensile stresses are present at interior locations. Equal triaxial tensions theoretically prevent any plastic flow or deformation and triaxial tensile stresses of any extent will suppress yielding to some degree thus promoting the possibility of a brittle fracture. The extent of triaxiality will be a function of notch and specimen geometry with the actual stress condition falling somewhere between plane stress and plane strain, although conditions in most structures more closely approximate plane strain.

Although a triaxial stress state can serve to inhibit general yielding, it has been fairly well established that some plastic deformation at the notch tip always precedes brittle fracture initiation, no matter how sharp the notch.[11] Since limited yielding does precede fracture initiation, the maximum stress will not necessarily occur at the notch tip as predicted by elastic theory, but rather at some finite distance beneath the notch surface at the midthickness of the plate. In order to study the initiation mechanism and the stresses associated with the onset of rapid fracturing, it then becomes necessary to consider the conditions at an interior point in a body--conditions which cannot all be determined experimentally, nor easily measured.

Because the stress state and stress distribution at the region of interest are at an interior point in a body, surface measurements alone will not suffice as a means of predicting these quantities. A mathematical approach must be employed to provide the necessary supplementary information. Because some plastic deformation always precedes fracture initiation, the mathematical technique used cannot rely solely on the theory of elasticity, but must include some theory of plastic deformation applicable to the yielded region. The particular stress analysis chosen must not only satisfy the appropriate equations of elasticity and plasticity but also must satisfy the boundary conditions.

The general procedure to be followed in the stress analysis of the problem is as follows: a model will be selected that will yield easily to mathematical analysis and also one which is similar to the experimental specimen to be analyzed. A complete elastic solution to the problem will then be obtained. In the elastic

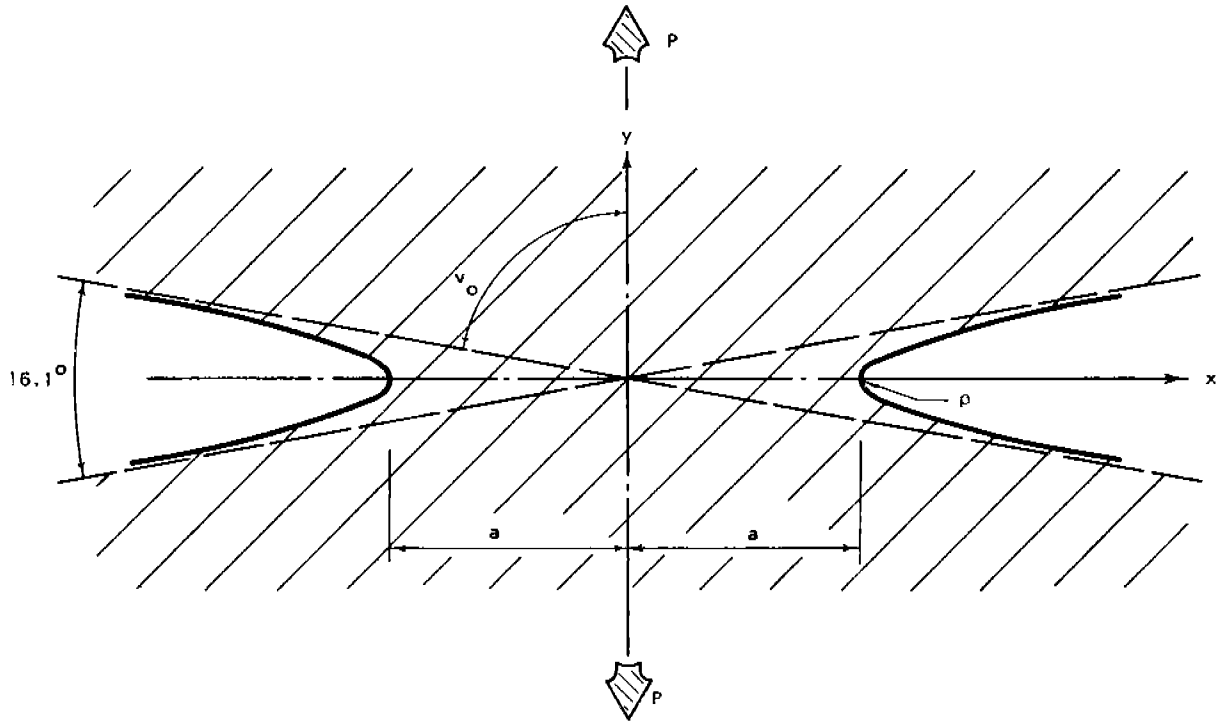

FIG. 1. ANALYTICAL MODEL.

analysis of the problem, the appropriate equations of elasticity will be solved at a discrete number of points in the exact continuous model. Once the elastic solution has been obtained, an approximate technique will be utilized to take into account any plastic deformation that would have occurred. The final results will then be obtained from the elastic-plastic stress analysis.

Model Used .

The model chosen for the stress analysis is a solid body whose cross-section is shown in Fig. 1. The geometry of the model was selected such that the dimensions of the cross-section in the region of the notch in the x-y plane corresponded to the cross-section and notch configuration used for the specimens in the experimental study. The body is assumed to be of infinite extent both in the x-y plane of the figure and also in a direction normal to that plane. Thus in this analytical study the problem to be considered is one of plane strain.

In both the elastic and elastic-plastic stress analysis, it is assumed that the material is homogeneous and isotropic throughout the body. The uniaxial tensile load, P, per unit thickness normal to the x-y plane acts in a longitudinal direction parallel to the y-axis. This load, which is applied in some manner at an infinite distance from the minimum cross-section, may also be expressed in terms of the average applied stress on the minimum cross-section, σ_A, by the relation $P = 2a\,\sigma_A$. All other surfaces are free of stress.

For convenience, dimensions have been assigned to the model which correspond to the dimensions of the experimental specimen. The total minimum section width, 2a, is equal to 1 in. and the root radius of the notch, ρ, was selected to be 0.01 in. The ratio of the half width at the minimum cross-section, a, to the radius of curvature of the root of the notch, ρ, is $a/\rho = 50$. The notch surfaces are formed by the two sheets of an hyperbola having an included angle of 16.1 degrees between asymptotes. With this particular specimen configuration of $a/\rho = 50$, the theoretical elastic stress concentration factor at the notch tip is approximately 9. The expression representing the notch surfaces in rectangular coordinates may be written as:

$$x^2/a^2 - y^2/a\rho = 1 \qquad (1)$$

Elastic Stress Analysis

The purely elastic stress analysis is considered first because it forms the foundation for the subsequent elastic-plastic stress analysis. For the elastic solution it is assumed that the material is perfectly elastic throughout and obeys Hooke's Law.

The solution to the elastic problem will be in the form of a stress function, φ, which will then define the stresses at any point in the body. The general form of the stress function is that developed by Neuber[1,2] in his stress analysis of elastic bodies with the same notch configuration and the same type of applied loading as used in this study. The general stress function as given by Neuber is:

$$\varphi = Axv + B \cosh u \cos v + C \qquad (2)$$

where A and B are constants to be determined from the boundary conditions and C is an arbitrary constant which may be used to set the value of the stress function to some convenient value at any desired point, such as the coordinate origin or notch root.

The general equations of elasticity must be satisfied by the stresses at every point in the body. Generally these consist of equilibrium equations, compatibility equations and the boundary conditions of the problem. The equilibrium equations may be satisfied by selecting an appropriate stress function, φ, (Airy stress function) such that the stresses may be expressed as,

$$\frac{\sigma_x}{\sigma_{ys}} = \frac{\partial^2\varphi}{\partial y^2}$$

$$\frac{\sigma_y}{\sigma_{ys}} = \frac{\partial^2\varphi}{\partial x^2} \qquad (3)$$

$$\frac{\tau_{xy}}{\sigma_{ys}} = -\frac{\partial^2\varphi}{\partial x \partial y}$$

where σ_{ys} is the yield stress in simple tension.
The compatibility requirements are satisfied providing that the stress function, φ, satisfies the equation

$$\nabla^4\varphi = \frac{\partial^4\varphi}{\partial x^4} + 2\frac{\partial^4\varphi}{\partial x^2 \partial y^2} + \frac{\partial^4\varphi}{\partial y^4} = 0 \qquad (4)$$

The boundary conditions of the problem may be summarized as follows: (1) the notch surfaces (free surfaces) must be free of stress; i.e., the normal and tangential stresses along the notch surface must equal zero ($\sigma_x = \sigma_y = \tau_{xy} = 0$). (2) the integral of the axial stress component (σ_y) across the minimum cross-section (along x-axis) of the body must be equal to the total applied load. Actually the integral of the axial component of stress across the body along any line y = constant must equal the applied load, but it will be shown later that satisfying this requirement along the minimum cross-section also insures that it will be satisfied along any line parallel to the x-axis.

Consider the first boundary condition:

$$\sigma_x = \sigma_y = \tau_{xy} = 0 \text{ (along notch surface)}$$

This condition requires that along the boundary (notch surface),

$$\frac{\partial\varphi}{\partial y} = \text{constant}$$

and (5)

$$\frac{\partial\varphi}{\partial x} = \text{constant}$$

These conditions are satisfied provided that

$$B = Aa \sin v_o \qquad (6)$$

The second boundary condition requires that the integral of the axial stress component across the minimum section must equal the applied load.

This boundary condition is satisfied by taking

$$A = \frac{a\,\sigma_A}{\sigma_{ys}\,(v_o + \sin v_o \cos v_o)} \qquad (7)$$

For convenience, φ at the notch tip was arbitrarily selected to be zero, and the constant C thus becomes:

$$C = -a^2\frac{\sigma_A}{\sigma_{ys}} \qquad (8)$$

The final form of the stress function, φ, which satisfies the equations of equilibrium, compatibility and the boundary conditions, is given as follows:

$$\varphi = -a^2 \frac{\sigma_A}{\sigma_{YS}} \left[1 - \cosh u \frac{(v \sin v + \sin^2 v_o \cos v)}{(v_o \sin v_o + \sin^2 v_o \cos v_o)}\right] \quad (9)$$

With the stress function defined for the problem under study, it is now possible to calculate all desired stresses for the elastic case. This was done by calculating the value of the stress function at a finite number of points arranged in the form of a regular x-y net, and calculating the desired stresses utilizing finite difference approximations instead of the exact differential expressions. The finite difference net selected was a square net with the lattice points equally spaced in both the x and y coordinate directions.

The values of the stress function at points within the net were calculated with the aid of the University of Illinois high-speed digital computer, the ILLIAC. The initial net spacing was arbitrarily selected to be d = a/16 (1/32 in.) since this seemed to provide a net with sufficiently small spacing, and at the same time did not result in an unreasonably large number of points. Because the model contained two lines of symmetry, it was necessary to calculate stress function values over only one-quarter of the specimen. The calculation of stress function values was limited to a region bounded by the lines x = 0, y = 0, x = 24d, y = 12d, since this would be the major region of interest in the elastic-plastic analysis. A sketch of this region of the net is shown in Fig. 2 (a).

Since the value of the stress function is dependent on the applied loading, an arbitrary ratio of $\sigma_A/\sigma_{YS} = 1$ was selected for use in the computer solution. Values of the stress function or subsequently calculated stresses could easily be obtained for other ratios of σ_A/σ_{YS} by applying an appropriate multiplication factor. The input values of coordinates to a point were given in terms of x and y and were transformed to corresponding values of u and v by the computer.

The accuracy of the stresses determined from the ILLIAC-calculated stress function values could easily be checked along the x-axis where σ_U and σ_V, available exactly from Neuber's closed form solution, were equivalent to σ_X and σ_Y. It was found that the approximate values of the stresses were considerably in error in the region of the notch

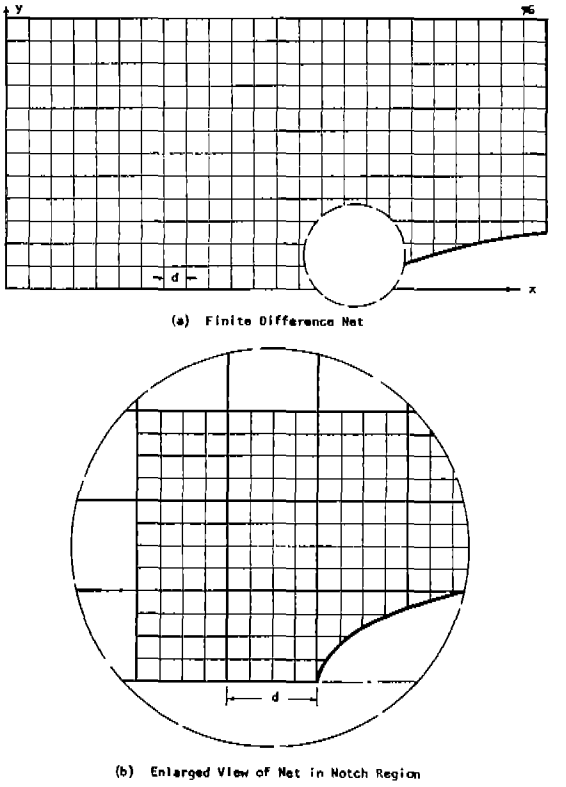

(a) Finite Difference Net

(b) Enlarged View of Net in Notch Region

FIG. 2. FINITE-DIFFERENCE NET USED IN ANALYSIS.

tip because of an inherent error in the calculation of arc sin v by the computer. The computer program was then modified so that the value of arc sin v could be calculated by hand. This eliminated any computer error in the calculation of the stress function and insured that any subsequent error in the calculated stresses was attributable primarily to the lattice spacing. A subsequent check of stresses as determined from the new exact stress function values indicated errors of less than 2 per cent except within a distance of 2d (2 lattice spacings) from the notch root. Within this distance, however, where the stress gradient was large, errors as large as 10 per cent in calculated stresses were observed.

Subsequent investigation revealed that the maximum error could be reduced to less than 5 per cent by refining the initial lattice net in the region of the notch by a factor of 4. And an error of this magnitude was noted only for node points immediately adjacent to the notch surfaces. Thus the new net spacing chosen was d' = d/4 = a/64. This grid refinement was carried out within a region bounded by x = 14d, x = 18d, y = 0, y = 3d. This refined region of the net is shown in Fig. 2 (b).

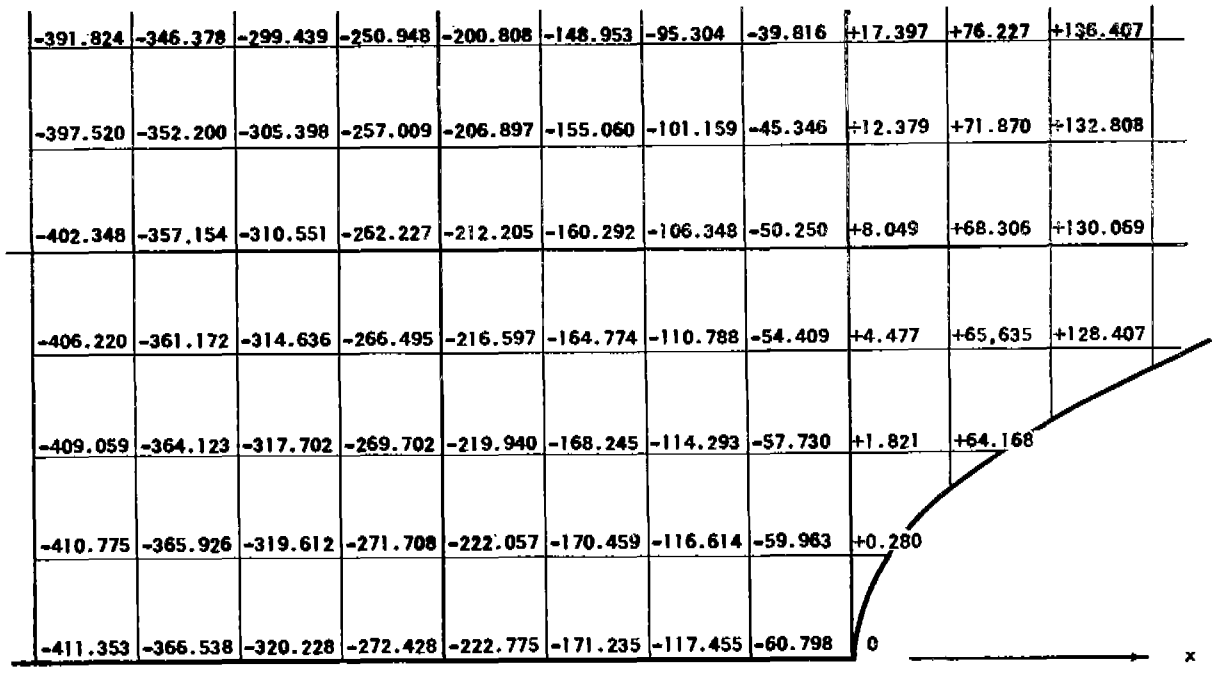

FIG. 3. ELASTIC STRESS FUNCTION VALUES FOR $\sigma_a / \sigma_{ys} = 1$, MULTIPLIED BY 16,384.

Values of the stress function at the additional points within the finer net were calculated in the same manner as described previously. Calculated values of the stress function for a ratio of $\sigma_A / \sigma_{YS} = 1$ are given in Fig. 3. With stress function values determined for each node in the lattice, stresses could be calculated at any desired point and the elastic analysis of the problem was now complete. The elastic distribution of σ_X and σ_Y along the minimum section is shown in Fig. 4.

Elastic-Plastic Stress Analysis

With the elastic solution forming the foundation, a more complete solution of the problem now requires some modification such that plastic deformation will be taken into account along with the resulting changes in stresses and stress distribution. In the elastic-plastic analysis, additional conditions must be imposed that were not required for the elastic solution. These basic assumptions are as follows:

(1) The material is assumed to be homogeneous and isotropic in the plastic region as well as the elastic region.

(2) The material is ideally elasto-plastic; i.e., the material obeys Hooke's Law only within the elastic region and the material is non-strain hardening.

(3) Plastic deformation begins when the stress state reaches a critical value defined by the selected yield criterion.

(4) The change in shape of the notch surface as a result of plastic deformation is negligible and has no effect on the solution of the problem.

In the initial formulation of this problem, several yield conditions were considered and the Von Mises criteria was selected for use in this investigation. In terms of the yield stress and the principal stresses, the Von Mises yield condition is

$$(\sigma_1 - \sigma_2)^2 + (\sigma_2 - \sigma_3)^2 + (\sigma_3 - \sigma_1)^2 = 2\sigma_{YS}^2 \qquad (10)$$

Since this analysis is concerned only with plane strain conditions, $\sigma_3 = \upsilon(\sigma_1 + \sigma_2)$, where υ is Poisson's ratio. Substituting for

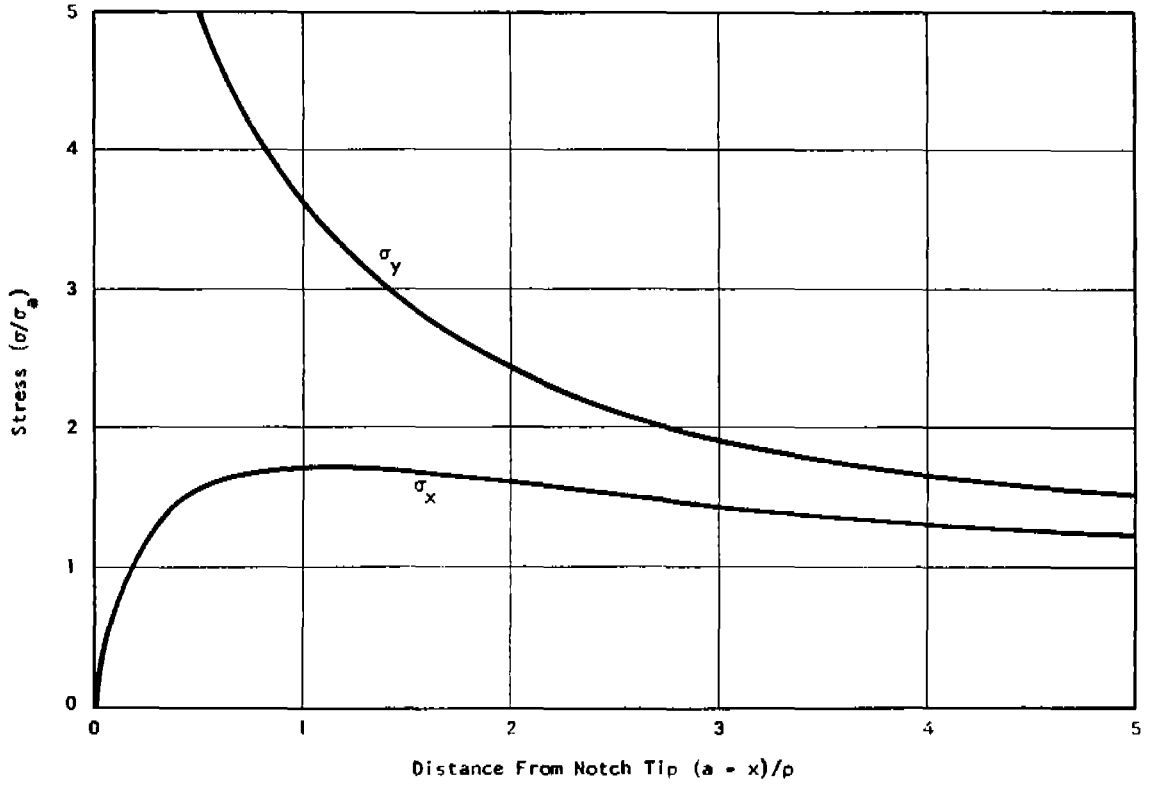

FIG. 4. STRESS DISTRIBUTION ALONG X-AXIS.

σ_3 in Eq. 10,

$$\sigma_1^2 (1 - \upsilon + \upsilon^2) + \sigma_2^2 (1 - \upsilon + \upsilon^2) - 2\sigma_1 \sigma_2 (1/2 + \upsilon - \upsilon^2) = \sigma_{ys}^2 \quad (11)$$

In order to simplify this expression, it is necessary to consider the behavior of the material after yielding. It can be shown (13) that during plastic flow Poisson's ratio increases from its value at the elastic limit of the material to a final value of $\upsilon = 1/2$, approaching this value asymptotically. Because of this, and since any consequent error may be expected to be small, in the expression of the yield condition, υ will be given the value of 1/2. Making this substitution in Eq. (11) yields:

$$(\sigma_1 - \sigma_2)^2 = 4/3\ \sigma_{ys}^2 \quad (12)$$

or, converted to rectangular coordinates:

$$(\sigma_y - \sigma_x)^2 + 4\tau_{xy}^2 = 4/3\ \sigma_{ys}^2 \quad (13)$$

Equation (13) may be expressed in terms of the stress function, φ, as follows:

$$\left[\frac{\partial^2\varphi}{\partial x^2} - \frac{\partial^2\varphi}{\partial y^2}\right]^2 + 4\left[\frac{\partial^2\varphi}{\partial x \partial y}\right]^2 = 4/3 \quad (14)$$

At this point, the formulation of the problem for the elastic-plastic stress analysis is complete. The equations of elasticity and the plastic equation, or yield condition, which must be satisfied in the elastic and plastic regions respectively, and the boundary conditions of the problem, have been derived in terms of the stress function, φ. For convenience these are summarized below.

(1) Differential Equation in Elastic Region:

$$\frac{\partial^4\varphi}{\partial x^4} + 2\frac{\partial^4\varphi}{\partial x^2 \partial y^2} + \frac{\partial^4\varphi}{\partial y^4} = 0 \quad (15)$$

(2) Differential Equation in Plastic Region:

$$\left[\frac{\partial^2\varphi}{\partial x^2} - \frac{\partial^2\varphi}{\partial y^2}\right]^2 + 4\left[\frac{\partial^2\varphi}{\partial x \partial y}\right]^2 - 4/3 = 0 \quad (16)$$

(3) Boundary Conditions:

$$\frac{\partial \varphi}{\partial x} = a \frac{\sigma_A}{\sigma_{ys}}, \quad \text{(along notch surface)} \qquad (17)$$

$$\frac{\partial \varphi}{\partial y} = 0$$

The complete solution of the elastic-plastic problem is ideally to find a stress function, φ, as a function of the coordinates x and y, which will satisfy Eqs. (15) and (16) in the elastic and plastic regions respectively, subject to the boundary conditions given by Eq. (17) and the requirement of continuity at the elastic-plastic boundary. Unfortunately, there are several difficulties involved in a direct solution to this problem. Equation (16) is non-linear and therefore the usual techniques available for the solution of linear equations are not applicable. Also the exact location of the elastic-plastic boundary is not initially known but is determined as a part of the solution. For problems of this type, no general methods are known by which solutions may be directly obtained analytically.

Problems of this same type have been solved, however, by utilizing a step-by-step numerical iteration technique known as the relaxation method, due to Southwell[14]. Allen and Southwell[13] applied the "method of systematic relaxation" to a class of problems involving plane elastic-plastic deformation similar to the problem under discussion. In a similar investigation, Jacobs[15] applied Southwell's relaxation procedure to the problem of plastic flow in a notched bar under tension. More recently, Hendrickson, Wood and Clark[10] utilized the relaxation procedure in the solution of elastic-plastic stress distribution in cylindrical notched specimens.

In the present problem, however, the net spacing required for a satisfactory representation of the steep stress gradients existing around the notch tip results in an excessively large number of points at which the elastic and plastic equations would have to be solved. A manual solution of the equation by the relaxation technique would be exceedingly lengthy for even one loading condition, and the work involved in solving the problem for several loading conditions would be prohibitive. It was found that even by using the ILLIAC, the University of Illinois high-speed computer, the time required for one solution would be excessive. The difficulties encountered in attempting to solve a problem of this type by relaxation methods emphasizes the need for a more direct, less involved, approximate analysis which would yield results compatible with those obtained from a more rigorous solution, and which would be easily adaptable to specimen configurations other than those considered in this study.

The elastic-plastic stress analysis developed herein is based on the elastic solution discussed in the preceding section. In this analysis, rather than finding the maximum stresses corresponding to a given loading condition, the maximum stresses are selected first and the actual load corresponding to these stresses is then calculated. As will be discussed later, the results obtained from this analysis are felt to give a reasonably accurate representation of the actual stresses existing at the instant of fracture.

The first step in the procedure was to define the stress distribution in the elastic portion of the specimen. In a similar study of the stresses in a body after elastic-plastic deformation by Hendrickson, Wood and Clark[10], it was found that although the magnitudes changed, the distribution of the stresses in the elastic region was approximately the same before and after limited plastic deformation. This observation was also made by Russian investigators[16] in a similar study in which they made the basic assumption that the stresses in the elastic region are given by the Neuber solution.

Since it is probably close to the true stress distribution, it is assumed in this investigation that after limited plastic flow the distribution of stresses in the elastic region is adequately described by the elastic solution discussed in the preceding section. The procedure for the remaining analysis entails defining the yield zone and the stress distribution within the plastic region and subsequently determining the actual applied load corresponding to this particular stress distribution.

Since the stresses at the elastic-plastic interface are the ones of primary interest and can be obtained from the elastic distribution, it is not necessary to define exactly the stress distribution within the plastic region. It will be sufficient to roughly approximate the plastic stress distribution of the axial stress since

it will be used only for determining the applied load on the specimen. The maximum value of the stresses can be determined at the elastic-plastic interface from the elastic solution, and the value of the axial stress at the root of the notch can be found from the yield condition. The value of the transverse stress, σ_x, at the root of the notch is of course zero. Whether the distribution of the axial stress between the elastic-plastic boundary and the notch root is parabolic or linear or is described by some more complex function will have a negligible effect on the subsequent calculation of the load carried across the minimum section by the plastic region. Hence for convenience and simplicity, the distribution of the axial stress between the elastic-plastic boundary and the notch root was assumed to be linear. By assuming a location of the yield zone, or a corresponding elastic stress distribution, the maximum stresses at the elastic-plastic boundary can be determined and the corresponding applied load found by integrating the axial stress across the minimum section.

To determine the stresses at the elastic-plastic boundary (or fracture origin), the first step was to arbitrarily select an initial applied load or corresponding ratio σ_A/σ_{YS}, assuming purely elastic behavior, which then defines a definite stress distribution in the elastic region. From the preceding elastic solution, the values of the stress function corresponding to the selected load could then be determined at every point within the lattice. For convenience, the first approximation of the applied load initially selected was the ratio $\sigma_A/\sigma_{YS} = 1$; this is the same ratio selected previously for use in the calculation of stress function values. Equations (15) and (16), the elastic and plastic equations, express the mathematical conditions of the problem at lattice points within the elastic and plastic region, respectively. The elastic equation Eq. (15), is initially satisfied at all points within the lattice since the elastic solution is used as a starting point. However, the plastic equation, which defines the condition for initial yielding, is violated at certain points within the body. The region defined by these points is the region of plastic deformation corresponding to the actual applied load which must be subsequently determined.

The region in which the plastic equation was violated was determined by computing the plastic residuals, R_P^1, at every lattice point in the vicinity of the notch tip. The plastic residual, R_P^1, is defined as follows:

$$R_\varphi^1 = \left[\frac{\partial^2\varphi}{\partial x^2} - \frac{\partial^2\omega}{\partial y^2}\right]^2 + 4\left[\frac{\partial^2\omega}{\partial x \partial y}\right]^2 - 1.333 \quad (18)$$

where the superscript, 1, denotes the value of the ratio σ_A/σ_{YS}; the values of R_φ^1 were computed first for the ratio, $\sigma_A/\sigma_{YS} = 1$. Since the values of the stress function, φ, are linear functions of the applied load, it was possible to calculate plastic residuals for other loadings directly from R_φ^1. The expressions for the plastic residual corresponding to typical loadings are shown below.

$$R_\varphi^{\frac{1}{2}} = 1/4 \left[R_\varphi^1 - 4\right]$$

$$R_P^{\frac{3}{4}} = 9/16 \left[R_\varphi^1 - 1.037\right]$$

$$R_\varphi^1 = \left[R_\varphi^1\right] \quad (19)$$

$$R_P^{\frac{3}{2}} = 9/4 \left[R_\varphi^1 + 0.741\right]$$

$$R_\varphi^2 = 4 \left[R_\varphi^1 + 1.000\right]$$

To determine the approximate extent and shape of the yield zone, the actual value of the plastic residual is not actually necessary since it is the sign of the expression of R_P that determines whether or not the plastic equation was violated at a point. A negative value for R_P at a point within the lattice indicates that the plastic equation has not been violated, and thus the point is within the elastic region; a positive value of R_P at a point denotes a violation of the plastic equation, indicating that the point lies within the plastic or yield region. A sketch of the yield regions for different applied loads is presented in Fig. 5.

The exact location of the elastic-plastic boundary along the minimum section was obtained graphically by plotting the computed values of R_P at lattice points along the notch line versus the location of the node. From this plot, the exact distance of the plastic front from the coordinate origin could be determined. This distance, x_p, is shown plotted against the first approximation of the load in Fig. 6.

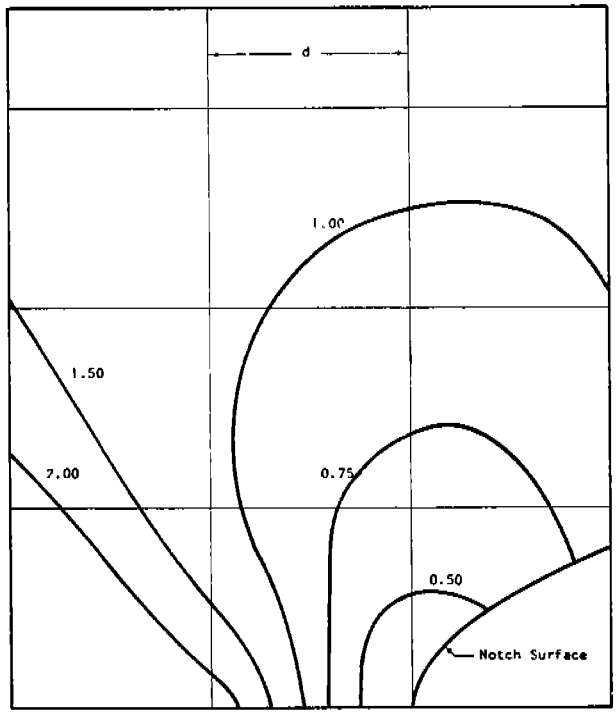

FIG. 5. TYPICAL YIELD REGIONS FOR VARIOUS VALUES OF σ_a/σ_{ys}.

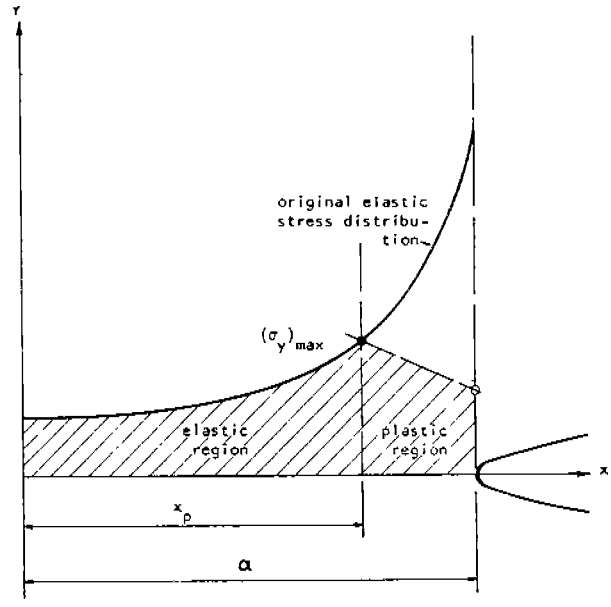

FIG. 6. LOCATION OF ELASTIC-PLASTIC BOUNDARY.

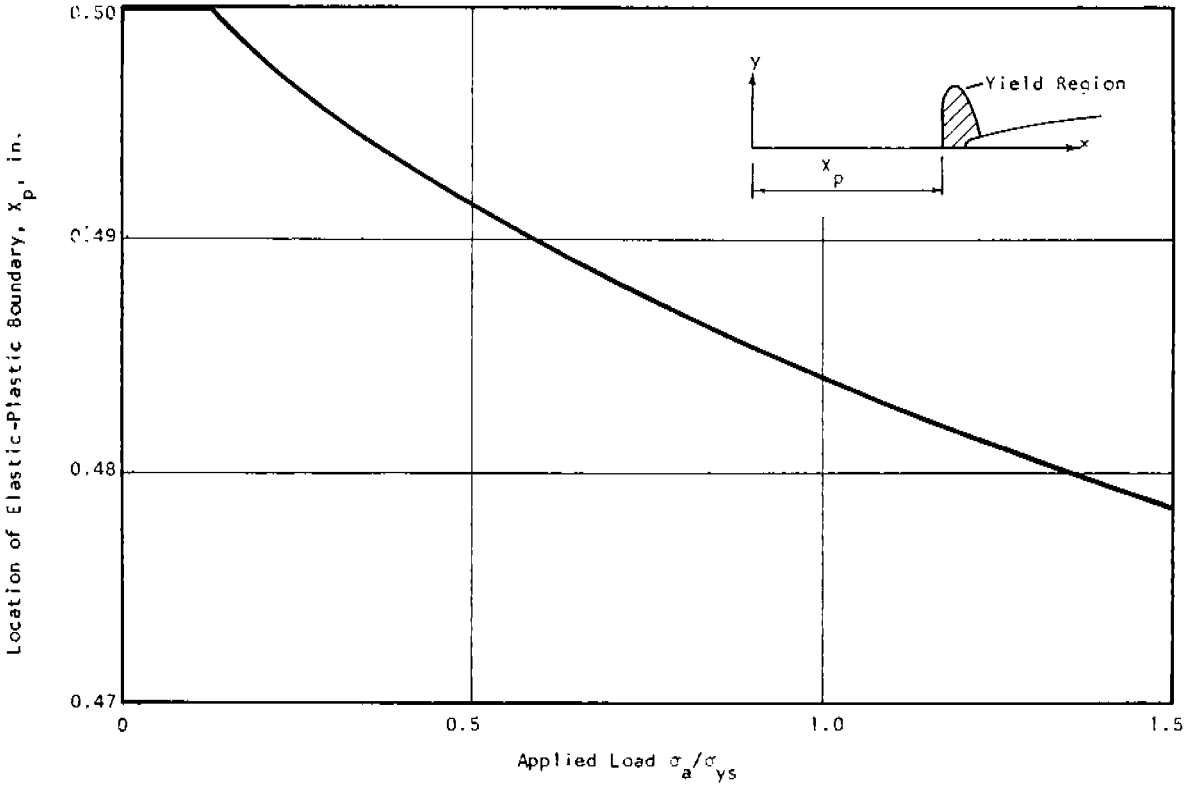

FIG. 7. STRESS DISTRIBUTION AFTER PLASTIC DEFORMATION.

The steps in finding the actual applied load after plastic deformation corresponding to a given yield region and elastic stress distribution are as follows. The initial assumed load defines the stress distribution in the elastic region and subsequently determines the location of the elastic-plastic interface, x_p, as indicated in Fig. 7. By integrating the axial stress across the elastic zone, the load carried by the elastic region can be found. The

axial stress at the elastic-plastic interface, which is the maximum axial stress, $(\sigma_Y)_{MAX}$, and the axial stress at the notch root determine the distribution of stress in the plastic region; thus the load carried by the plastic region can be found. The actual load is the sum of the loads carried by the elastic and plastic regions; the stress distribution corresponding to this load is as shown in Fig. 7. The final load corresponding to a particular extent of plastic deformation, x_p, will always be slightly less than the first approximation to the load from which x_p was first obtained.

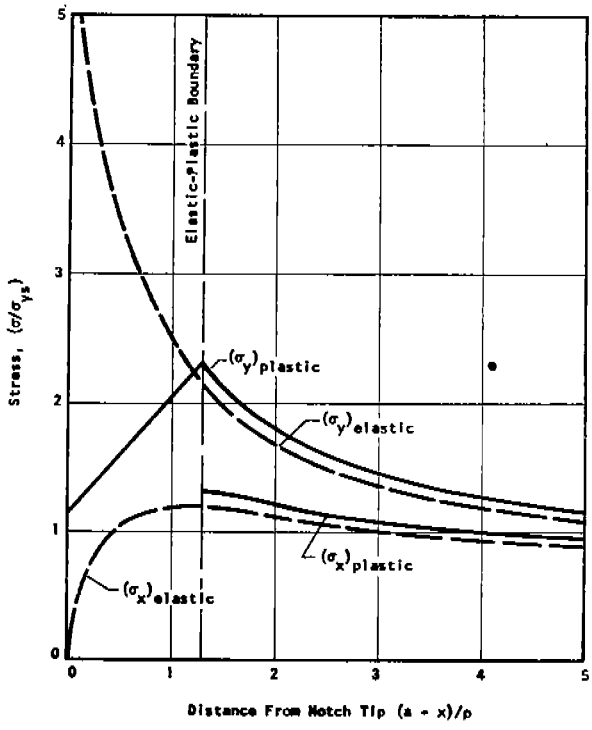

FIG. 8. ELASTIC AND ELASTIC-PLASTIC STRESS DISTRIBUTION ALONG MINIMUM SECTION FOR $\sigma_a/\sigma_{ys} = 0.70$

The principal stresses at the minimum cross-section are shown as a function of their location near the root of the notch in Fig. 8 for an applied load corresponding to a ratio $\sigma_A/\sigma_{YS} = 0.70$. For comparison, the stress distributions for elastic-plastic and purely elastic deformation are shown in this figure. The maximum axial stress, $(\sigma_Y)_{MAX}$, occurs at the elastic-plastic boundary and the values of $(\sigma_Y)_{MAX}/\sigma_{YS}$ as a function of $(\sigma_A/\sigma_{YS})_{ACTUAL}$ are given in Fig. 9. Corresponding values of $(\sigma_X)_{MAX}/\sigma_{YS}$ and $(\sigma_Z)_{MAX}/\sigma_{YS}$ as functions of σ_A/σ_{YS} are presented in Figs. 10 and 11 respectively.

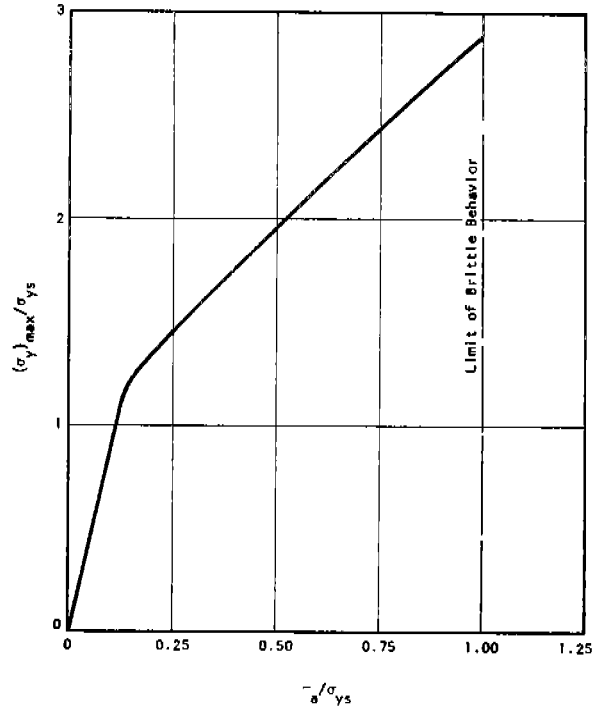

FIG. 9. MAXIMUM AXIAL STRESS $(\sigma_y)_{max}$ vs. APPLIED LOAD.

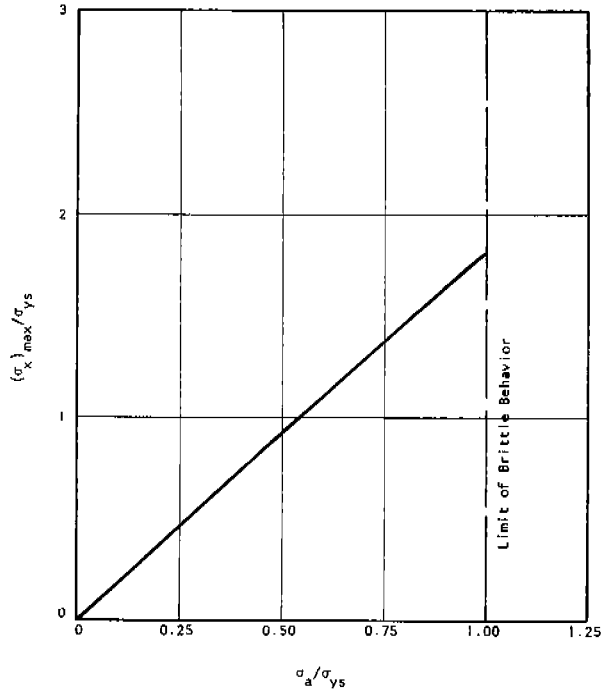

FIG. 10. MAXIMUM TRANSVERSE STRESS $(\sigma_x)_{max}$ vs. APPLIED LOAD.

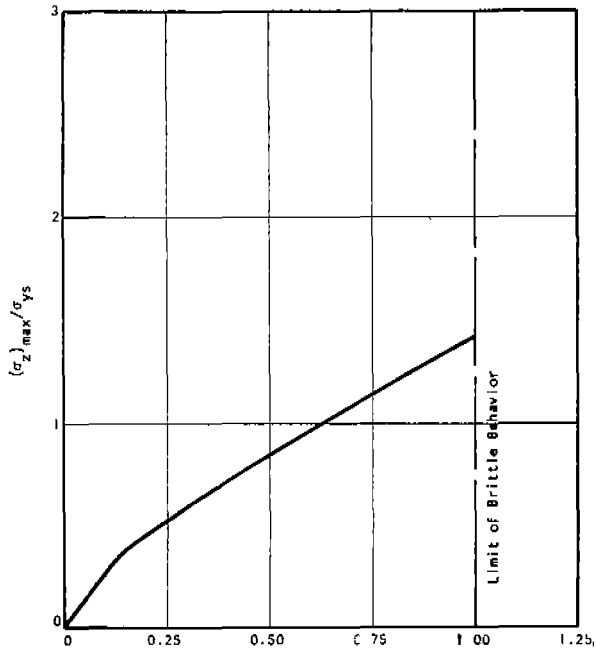

FIG. 11. MAXIMUM STRESS IN THICKNESS DIRECTION, $(\sigma_z)_{max}$ vs. APPLIED LOAD.

For the particular notch used in this investigation, the elastic stress concentration factor is 9.014. The yield condition employed is such that at the root of the notch where $\sigma_X = 0$, σ_Y always has the value of 1.154 σ_{YS} or $\sigma_Y/\sigma_{YS} = 1.154$. For purely elastic deformation, the axial stress at the root of the notch is $\sigma_Y = 9.014\ \sigma_A$. Thus the applied load at which yielding just begins is $\sigma_A/\sigma_{YS} = \frac{1.154}{9.014}$, or $\sigma_A/\sigma_{YS} = 0.128$. Obviously $(\sigma_Y)_{MAX}/\sigma_{YS}$ also equals 1.154. Thus for values of $\sigma_A/\sigma_{YS} < 0.128$, all deformation in the body is elastic, while for loads such that $\sigma_A/\sigma_{YS} > 0.128$, some plastic deformation occurs in the region of the notch root. For increasing loads, the extent of the region of plastic deformation also increases until a load is reached at which yielding has extended from the notch root to the axis of the specimen. Since the analysis described is valid for only limited plastic deformation and since brittle behavior was of primary interest, it was necessary to define an upper limit to the applied load for which the region of plastic deformation was limited to the immediate vicinity of the notch tip.

An examination of the yield regions for different loadings indicated that for $\sigma_A/\sigma_{YS} < 1$, the shape of the plastic regions were similar and were confined to the notch region. For $\sigma_A/\sigma_{YS} > 1$, however, the region of plastic deformation began extending toward the axis of the specimen above and below the notch line as indicated in Fig. 5. This same behavior was noted by Allen and Southwell[18] and also by Hendrickson, Wood and Clark[10] in similar investigations. Thus for the particular conditions of this study, the extension of plastic deformation becomes unstable for an applied load corresponding approximately to $\sigma_A/\sigma_{YS} = 1$, and further increase in load will result in gross yielding of the specimen.

A consistent definition of brittle, as opposed to ductile, fracture in notched specimens can now be made on the basis of the foregoing discussion; this same basis of definition was used by Hendrickson, Wood and Clark[10] in their study of brittle fracture initiation. Any fracture, which occurs in the notched specimens used in this investigation, is defined as a brittle fracture if the applied load at fracture is such that $(\sigma_{AF}/\sigma_{YS}) < 1$. Conversely, any fracture which occurs after extensive plastic deformation, i.e., $(\sigma_{AF}/\sigma_{YS}) > 1$, is defined as a ductile fracture.

The results of this analytical phase of the investigation provide a method for determining the maximum principal stresses existing in the region of the notch at the instant of fracture initiation. These stresses can be calculated provided that the nominal stress at fracture, σ_{AF}, and the yield stress, σ_{YS}, are known.

EXPERIMENTAL INVESTIGATION

General

The purpose of this phase of the investigation was to study experimentally the initiation of brittle type fractures in flat plate specimens. Specifically, it was desired to determine the yield stress of the material at given temperatures, the nominal stress on the minimum section at fracture, and to evaluate the effect of specimen thickness and test temperature on the fracture behavior.

The values of yield stress and nominal fracture stress, as determined in these tests, were used directly in conjunction with the analytical stress solution to provide a picture of the stress state existing in the specimen at the

instant of fracture. The remainder of the experimental measurements recorded during the tests were used to provide a qualitative description of the behavior of the specimens during loading to fracture, such as the general deformation characteristics and the type of fracture at given test conditions.

Material Properties

The material used in this investigation was a semikilled, as-rolled steel manufactured by Bethlehem Steel Company (Heat No. 60B528). Although a heat-treated steel might possibly have given more consistent results, an as-rolled mild steel was selected since it is precisely this material in which a satisfactory explanation of the brittle fracture phenomenon seems most elusive. A check analysis of the material is included in Table 1.

Standard tensile tests were conducted at temperatures of 78 F, -100 F and -320 F, the same temperatures at which fracture specimens were tested. At room temperature, the upper-yield point of the material was 30 ksi and the ultimate stress was 58.6 ksi. A summary of the tensile test data is presented in Table 1. The variation of the yield strength and ultimate strength of the material as a function of temperature is shown in Fig. 12.

Charpy V-notch impact tests were conducted over a range of temperatures from -40 F to 140 F and also at -320 F; all Charpy specimens were parallel to the direction of rolling. The 15-ft-lb Charpy V-notch temperature was approximately 60 F as may be seen from Fig. 13. The energy absorbed at -40 F was approximately 4.0 ft-lbs and at -320 F, the energy absorbed was approximately 3.5 ft-lbs.

Specimen Description

The specimens used in this study were all machined from the same 1-in. thick plate. The overall width of each specimen was 2 in. and the edge notches were 1/2 in. deep resulting in a minimum section width of 1 in. Nominal specimen thicknesses used were 1/4 in., 1/2 in., 3/4 in. and 1 in. although the 1-in. specimen, after machining, had an actual thickness of approximately 0.9 in. Preparation of the specimens were such that the middle plane of the specimens coincided with the middle plane of the parent plate. A sketch of the specimen configuration is presented in Fig. 14.

TABLE 1. MATERIAL PROPERTIES.

A. Tensile Test Data (Standard ASTM 0.505-in. Diameter)*

Temperature °F	Upper Yield Stress (ksi)	Ultimate Stress (ksi)	Elongation in 2 in. %	Reduction in Area %
+78	30.0	58.6	46	67.0
-100	43.6	70.3	35	65.0
-320	114.2	114.8	0	0

* (All specimens parallel to direction of rolling--each value represents average of two tests.)

B. Check Analysis

C	Mn	Si	P	S	Ni	Cr	Cu	Al
0.18	0.82	0.03	0.018	0.028	0.03	0.04	0.06	0.02

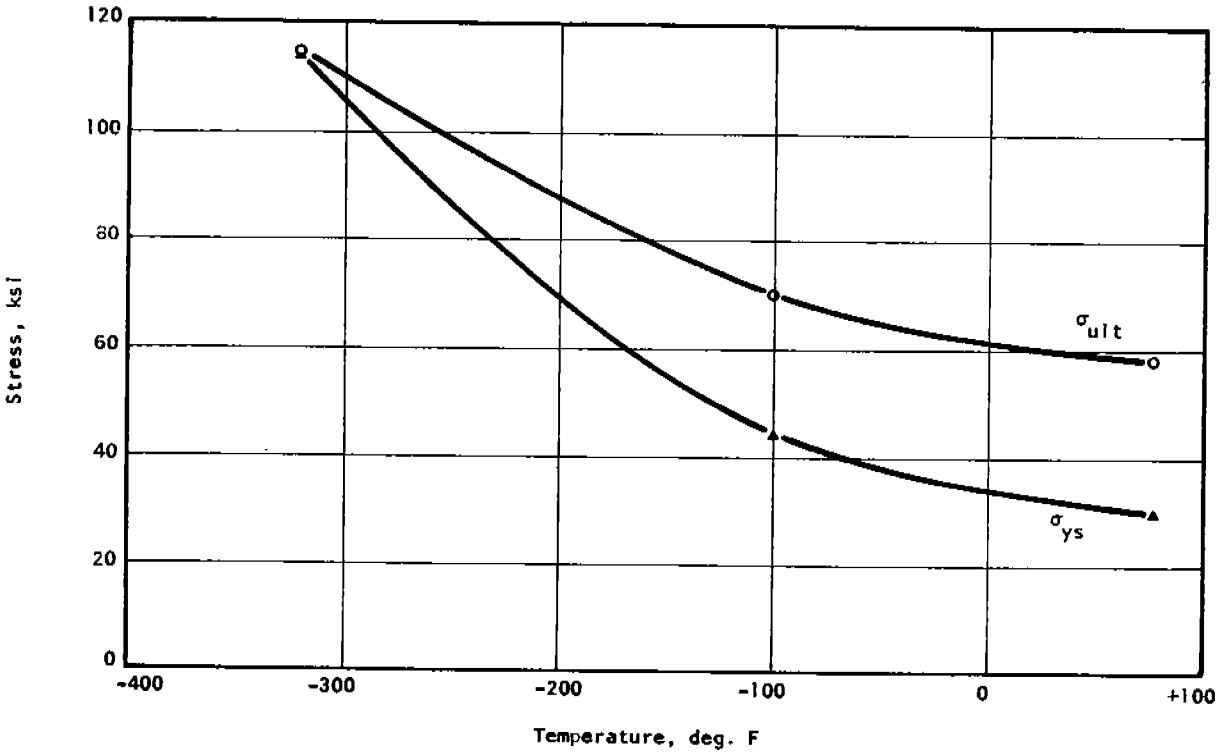

FIG. 12. YIELD AND ULTIMATE STRESS vs. TEMPERATURE.

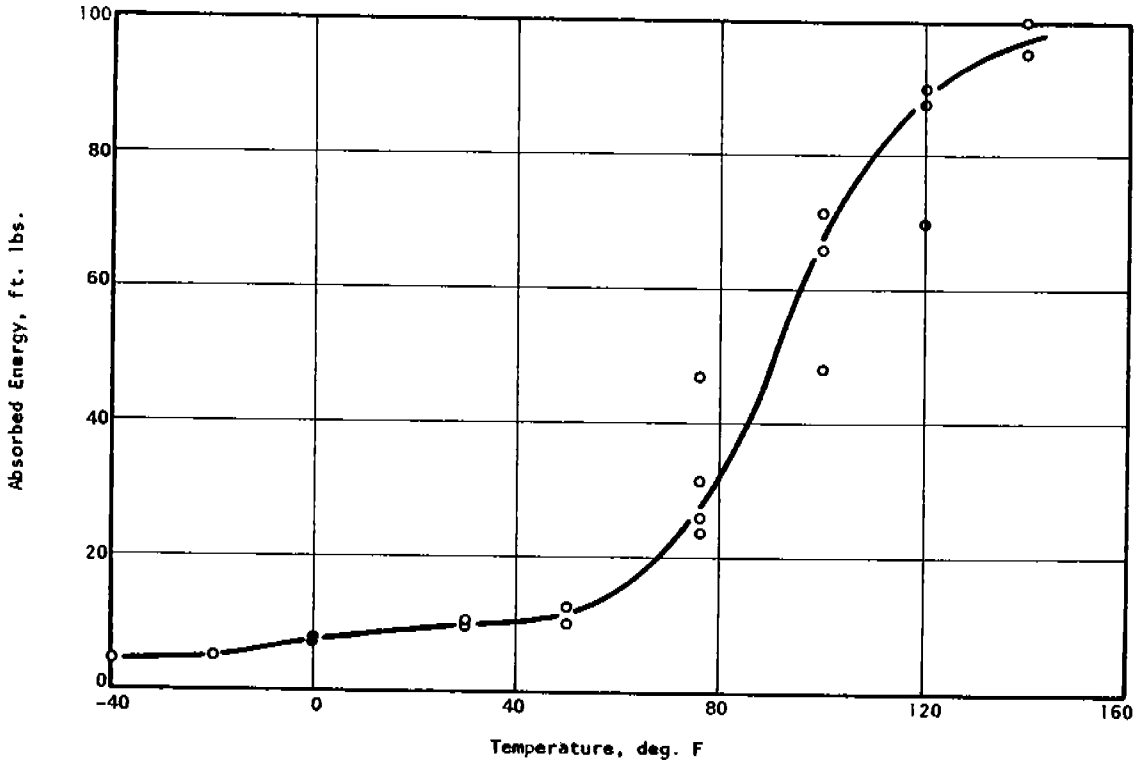

FIG. 13. RESULTS OF CHARPY V-NOTCH IMPACT TESTS.

The notch configuration selected was such that the notch surfaces were formed by the two sheets of an hyperbola as indicated in Fig. 14. The minimum radius of curvature at the notch tip was 0.01 in., resulting in a theoretical elastic stress concentration factor of approximately 9. This particular notch configuration was selected so that the geometry of the experimental specimen would correspond as closely as possible to the geometry of the model used in the analytical study.

All specimens were prepared with their longitudinal axis parallel to the direction of rolling. The surfaces of the specimens were machined and polished to the desired dimensions. The notch was machined in the specimen edges using a milling cutter manufactured especially for this particular series of tests. A comparison of the shape of the machine notch with the theoretical shape indicated that the maximum difference between the two was less than 0.001 in.

Test Procedure and Equipment

All tests, with the exception of a few preliminary pilot tests, were conducted in a

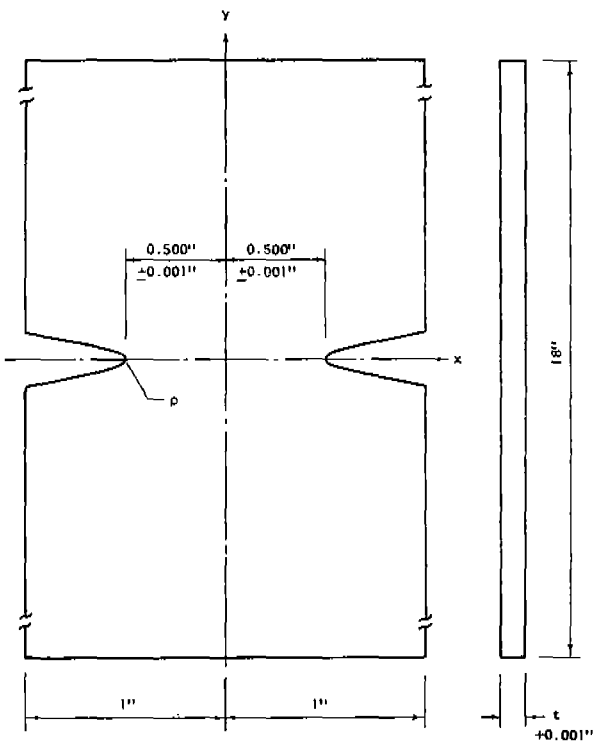

FIG. 14. SPECIMEN AND NOTCH DETAILS.

120,000-lb-capacity hydraulic testing machine. The general test procedure consisted of instrumenting the specimens, cooling to the desired temperature for low temperature tests, and loading to fracture.

Tests were conducted at room temperature, -100 F and -320 F; room temperature was approximately 78 F. The test temperature of -100 F was obtained by placing alcohol and dry ice into a container and pumping the cooled alcohol through a closed cooling tank surrounding the test section, with regulated flow for temperature control. The test temperature of -320 F was obtained using the same cooling tank except that liquid nitrogen was pumped through the cooling system. In this case, pumping was accomplished by introducing nitrogen gas under pressure into the flask containing the liquid nitrogen; the rate of flow was controlled by adjusting the pressure of the gas. To achieve the temperatures of -100 F and -320 F it was necessary to circulate the cooling agent such that it was in direct contact with the specimen.

The temperature on all specimens was determined by means of copper-constantan thermocouples mounted on the specimen surface in the vicinity of the notch. Readings from thermocouples placed on the transverse center line and 3/8 in. above and below this line indicated a negligible gradient in both the longitudinal and transverse directions. The maximum temperature variation for all tests conducted at a given temperature was approximately ±5 F, and was not considered large enough to have any significant effect on the test results.

The loading rate used for all tests was maintained at a sufficiently low value so that all tests could be considered as static tests. All loading was applied in an increasing manner so that no unloading occurred and thus stress history could be eliminated as a variable. On room temperature tests in which strain gages were employed, loading above the yield point was done in increments, with a particular load level being held until yielding stopped and the strain gage readings became stable. For all other tests, loading was continuous.

Instrumentation and Measurements

Before and after testing, the exact dimen-

sions of the minimum section of each test specimen were carefully measured using a micrometer and depth gage which gave measurements directly to within 0.001 in. and permitted estimated measurements to the nearest 0.0005 in.

Temperature-compensated foil strain gages were used on representative specimens of each thickness tested at room temperature and at -100 F. The gages were oriented vertically and horizontally along the notch line, with each pair of vertical and horizontal gages located back-to-back on opposite faces of the specimen at the notch tip and specimen centerline.

Specimen extension in room temperature tests was also determined by means of a 2-in. extensometer, which permitted a check on the strains obtained from the strain gages. The extensometer was made specifically for this series of tests and utilized a 4-arm bridge arrangement to measure extensions.

Test Results

The average fracture stress, σ_{AF}, in all tests was determined by dividing the fracture load by the original area of the minimum cross-section. This introduced relatively little error since, with only two exceptions, all fractures, even at room temperature, were of a cleavage nature and the final area at the time of fracture was not substantially different from the original area. Apparently, temperature did not have a significant effect on the value of the average fracture stress as can be seen in Fig. 15. The average fracture stress at all test temperatures was approximately 68 ksi.

Within the range of specimen dimensions included in this study, the variation in thickness was apparently insufficient to indicate any significant effect of thickness on fracture stress, especially at the lower temperatures. The only indication of any thickness effect was in the mode of fracture of specimens tested at room temperature. The 1/4-in. thick specimens and one 1/2-in. specimen failed by shear after undergoing extensive yielding, while all remaining specimens of 1/2-in. or greater thickness, tested at room temperature, and all specimens tested at lower temperatures failed by cleavage.

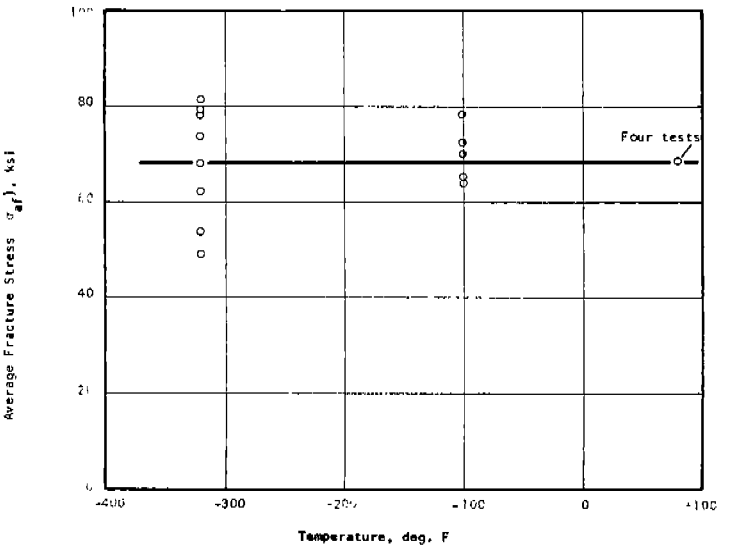

FIG. 15. AVERAGE FRACTURE STRESS vs. TEMPERATURE.

The relationship between the average applied stress on the minimum section, σ_A, and the deformation of the specimen under load was obtained from strain gage measurements and limited extensometer data. It was found that the deformation behavior of a specimen was essentially the same at a given temperature regardless of thickness. The relations between average minimum section stress and longitudinal and transverse strain, at the center-line and notch root of a typical notched specimen tested at room temperature, are shown in Figs. 16 and 17, respectively. Also shown in Fig. 16 is the longitudinal strain at the center-line as determined from extensometer data. Although the extensometer gage length was considerably greater than that for a strain gage, it can be seen that the strain behavior as determined by the two types of measurements are essentially the same. Similar relationships between average stress across the minimum section and surface strains for a typical

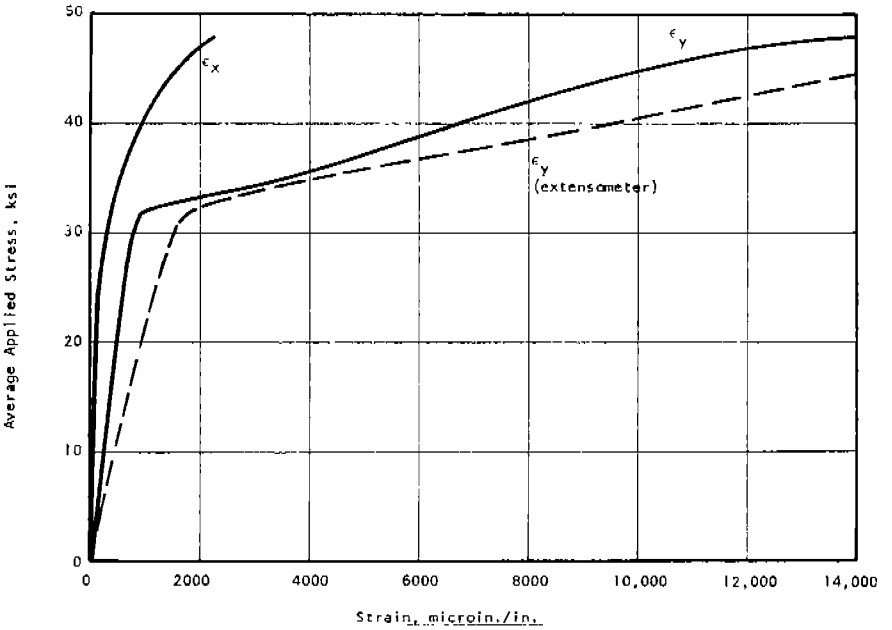

FIG. 16. AVERAGE STRESS vs. STRAIN MEASURED AT CENTER-LINE AT +78 F.

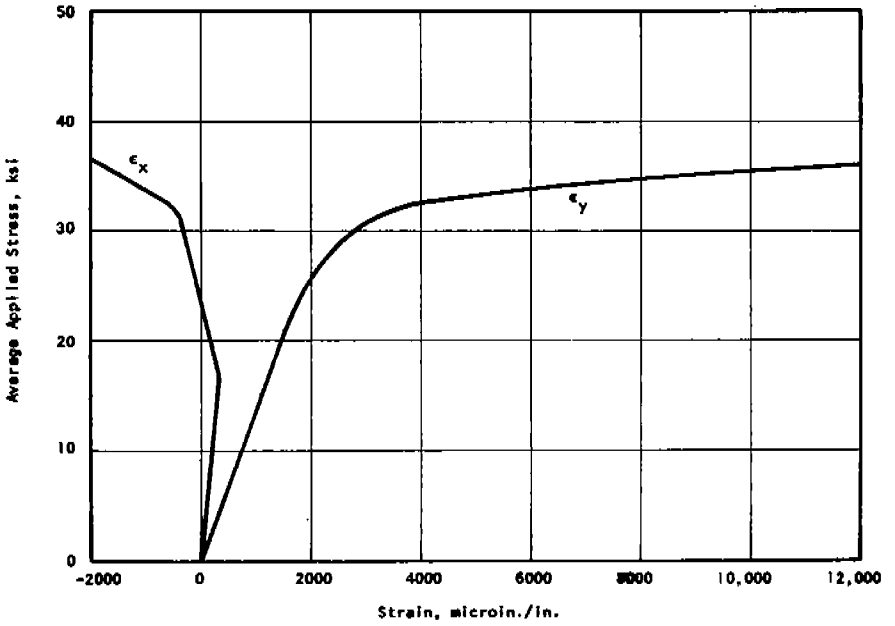

FIG. 17. AVERAGE STRESS vs. STRAIN MEASURED AT NOTCH TIP AT +78 F.

specimen tested at -100 F are presented in Figs. 18 and 19. Although strain gage data at -100 F could not be obtained once yielding had commenced, a comparison of the previous stress-strain diagrams indicate that initial yielding occurred at a somewhat higher value of applied load for the specimen tested at -100 F.

The relationship between reduction in thickness measured after fracture and the temperature is shown in Fig. 20 and Fig. 21 for measurements made at the center-line and notch tip respectively. The average reduction in thickness at the specimen center-line for all specimens tested at room temperature was approximately 10 per cent, while at the notch tip reduction in thickness was roughly 19 per cent for 1/2-in. thick specimens and 13 per cent for the remainder. At liquid nitrogen temperature, the reduction in thickness at all points along the minimum section was negligible. Measurements from 1/4-in. specimens were not included because of the limited data

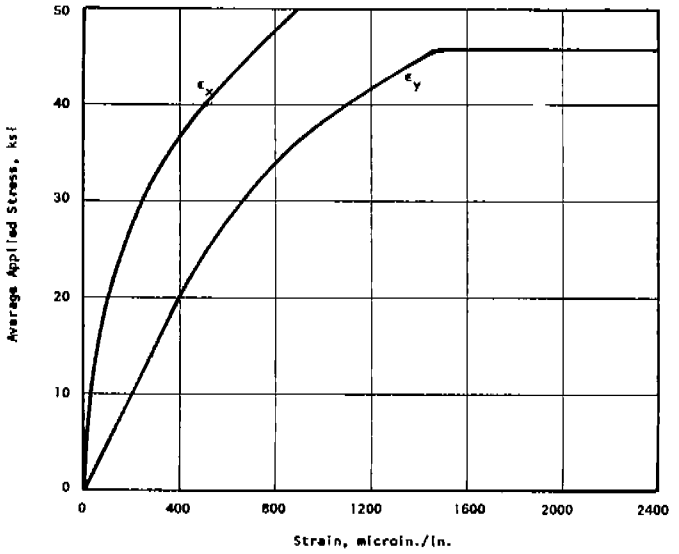

FIG. 18. AVERAGE STRESS vs. STRAIN MEASURED AT CENTER-LINE AT -100 F.

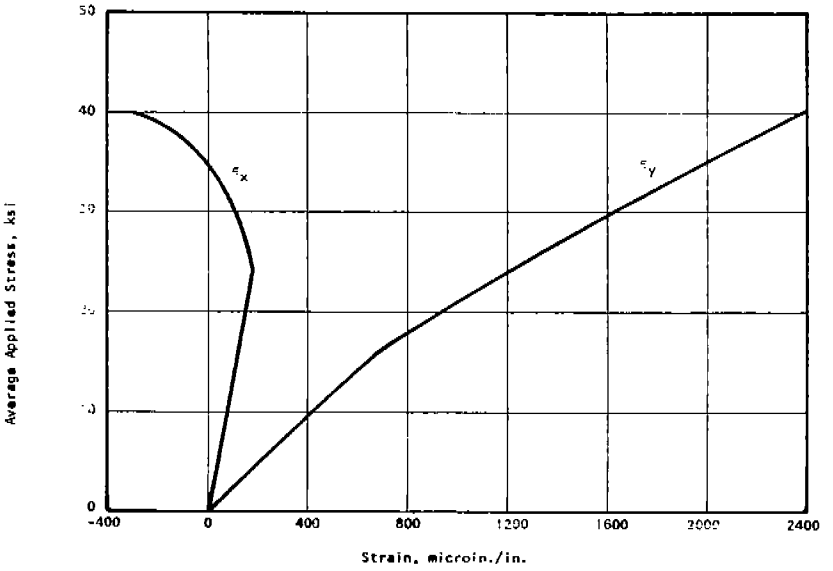

FIG. 19. AVERAGE STRESS vs. STRAIN MEASURED AT NOTCH TIP AT -100 F.

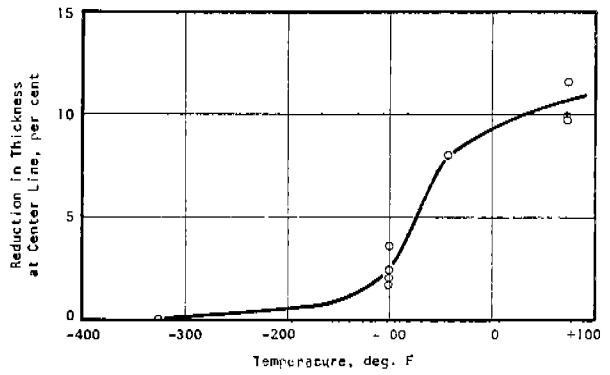

FIG. 20. REDUCTION IN THICKNESS AT CENTER-LINE vs. TEMPERATURE.

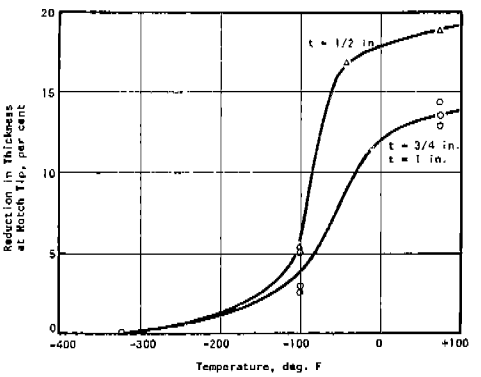

FIG. 21. REDUCTION IN THICKNESS AT NOTCH TIP vs. TEMPERATURE.

available as a result of shear failures at room temperature, but apparently reduction in thickness for these specimens would have been slightly greater at -100 F but negligible at -320 F. The variation in the reduction of thickness along the minimum section is shown in Fig. 22 for typical specimens tested at room temperature and at -100 F.

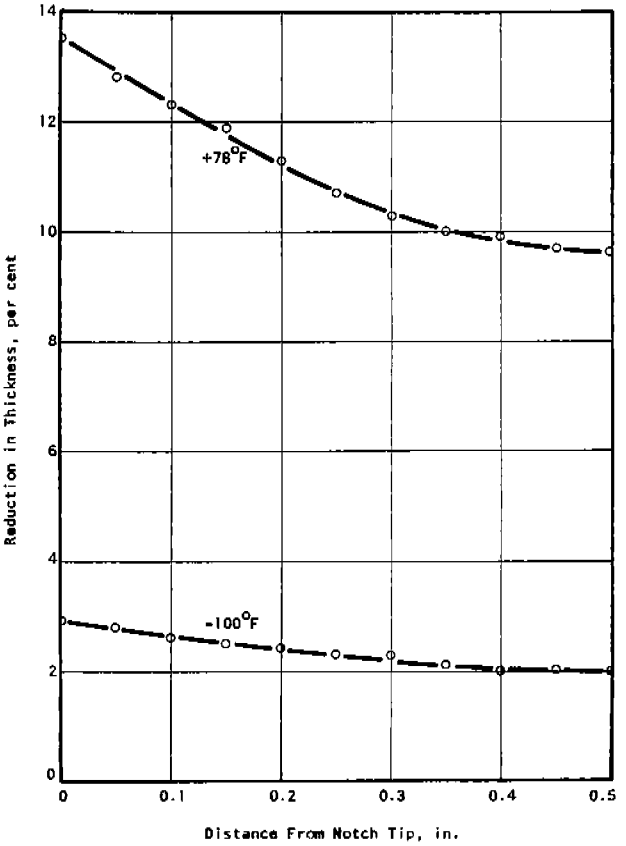

FIG. 22. TYPICAL REDUCTION IN THICKNESS ALONG MINIMUM SECTION.

As mentioned earlier, the fracture mode for all specimens tested at -100 F and -320 F was of a cleavage type and little difference could be noted in fracture appearance. A photograph of two typical fractured specimens tested at -100 F and -320 F are shown in Fig. 23. At room temperature, the dividing line separating cleavage fractures from shear fractures was apparently a specimen thickness of 1/2-in.; all specimens less than 1/2-in. thick failed in shear while specimens more than 1/2-in. thick failed by cleavage. Of the two 1/2-in. specimens tested at room temperature, one failed in shear and the other fractured in a cleavage manner. Photographs showing the fracture surface of these two specimens are presented in Fig. 24. All specimens which failed by cleavage at room temperature exhibited a small shear lip or thumbnail immediately adjacent to the root of the notch as may be observed from Fig. 24 (b). The remainder of the fracture surface had the general appearance of a brittle type fracture. However, in all room temperature tests, a noticeably large amount of plastic deformation preceded fracture, so these fractures could not be classified as brittle.

ANALYSIS AND DISCUSSION OF RESULTS

General

An approximate analytical elastic-plastic stress analysis for a plane-strain model, and the results of an experimental study utilizing a specimen of identical geometry except for a finite specimen width and thickness have now been presented. In order to determine the stresses existing at the location and instant

of fracture, it is necessary to combine the results from the analytical and experimental phases of this investigation.

It should be kept in mind that all results arising from this study were obtained from one particular specimen geometry and one material and although some of the results may be generally applicable, it is probable that they are valid only for the mild steel employed.

Limitations of Analysis

Before proceeding further, it is necessary to consider the limitations of the elastic-plastic stress analysis and to examine the justification for combining experimental results with an analytical stress analysis. The stress analysis in this study is developed for plane-strain deformations and stresses,

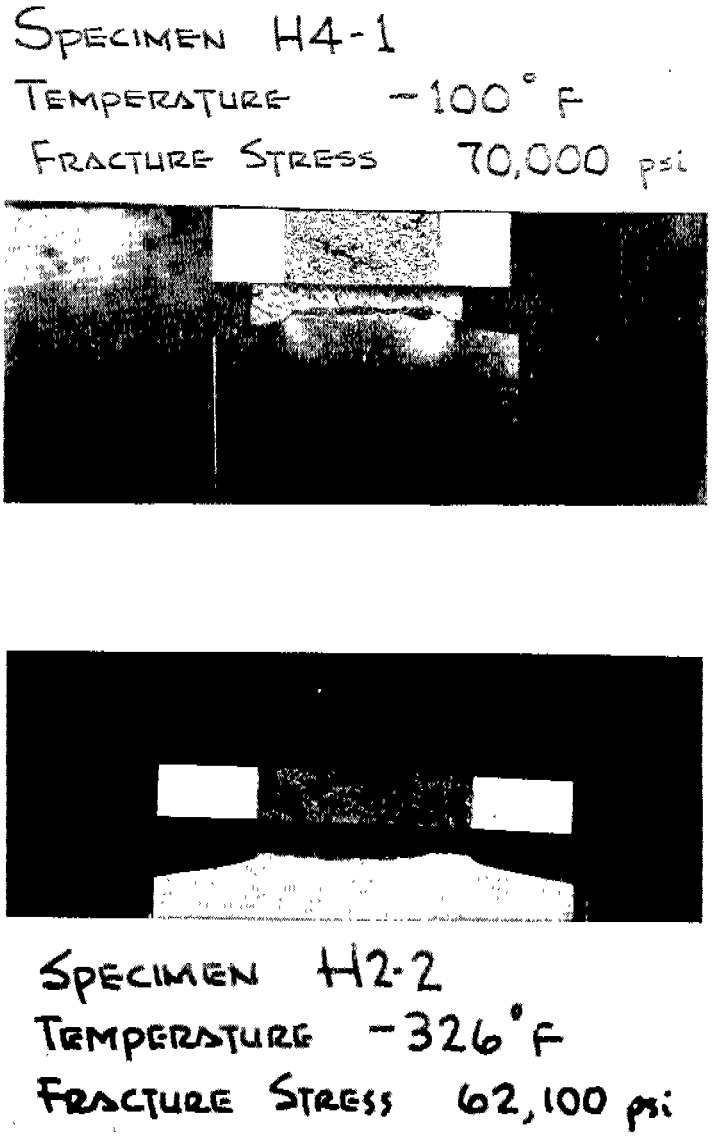

FIG. 23. TYPICAL FRACTURE SURFACES FROM TESTS AT -100 F and -320 F.

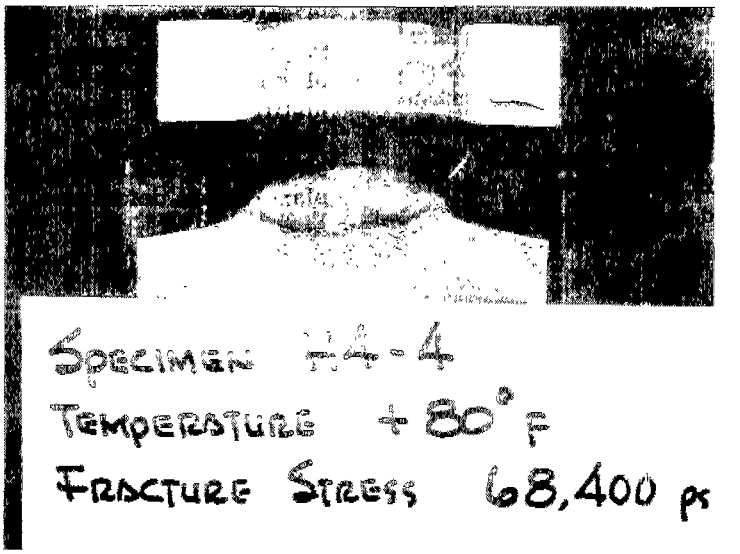

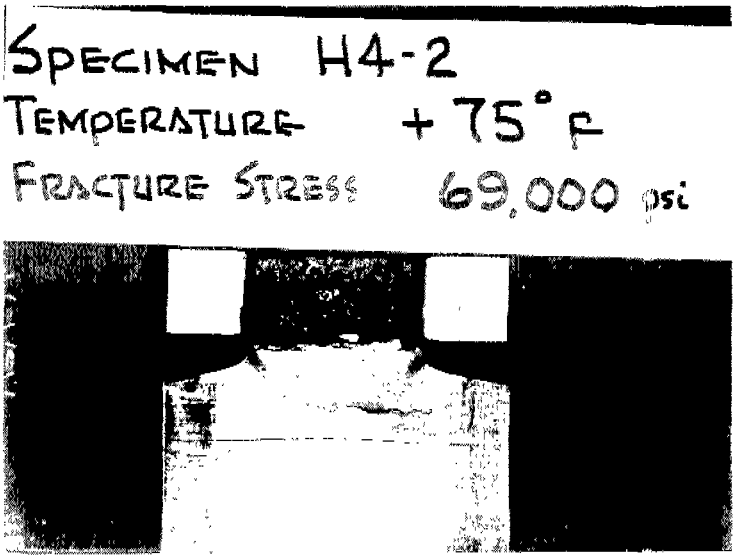

FIG. 24. FRACTURE SURFACES OF 1/2-in. THICK SPECIMENS TESTED AT +78 F.

although it is equally applicable to plane stress. The test specimens, on the other hand, have finite dimensions and thus the corresponding deformations will be neither plane strain nor plane stress, but somewhere in between. However, based on the results of this investigation, and on the results reported by other investigators, it is reasonable to assume that the actual state of stress in the test specimens employed in this study more closely approximates the condition of plane strain than plane stress. In fact, at the middle surface (mid-thickness) of a specimen, it may well be that a condition of plane strain does exist.

In the experimental study it was observed that specimens greater than 1/2-in. thick fractured by cleavage at room temperature, and at the lower test temperatures, specimens of all thicknesses fractured by cleavage. This is certainly an indication that sufficient restraint was present to prevent shear failures which would be expected for plane stress conditions. A further substantiation of the plane strain assumption may be found in the work of Sternberg and Sadowsky.[17] These investigators found that for a circular hole of diameter D, in an infinite plate of thickness t, the maximum stress σ_z, normal to the plane of the plate, approached the plane strain value of σ_z asymptotically as the ratio t/D increased. For the cases considered in their study, it was observed that σ_z at mid-thickness had, for all practical purposes, attained the plane strain value for ratios of t/D greater than 2. In the present study, the root radius of the hyperbolic notch was 0.01 in. and the smallest thickness employed was 0.25 in. Thus at the tip of the notch the ratio t/D would be approximately 12. It would therefore be reasonable to expect plane strain conditions to exist at the mid-thickness of the specimen in the vicinity of the notch tip, which is the primary area of interest in this investigation.

All results from the stress analysis are developed as a function of the average applied stress and the yield stress. For application of the stress analysis to a particular test specimen resulting in quantitative answers, it is necessary that the values of applied stress and yield stress be known. The average applied stress can usually be determined directly for a given specimen from the testing apparatus, but the yield stress must be determined separately as a function of rate of loading and temperature. In this study, the yield stress was determined for the specimen material from standard tensile tests conducted at the various test temperatures. A gradual rate of loading (static) was maintained throughout the test series and it was assumed that the yield stress as determined from tests on unnotched tensile specimens would also be the yield stress in the notched test specimens. Other investigators[9] have found that in static tests of notched specimens, yielding will occur at a maximum axial stress of about the same value as the static upper yield stress in unnotched specimens of the same material. Thus for every notched specimen tested in the experimental phase of this investigation, it was possible to compute the ratio of measured average stress at fracture to yield stress σ_{AF}/σ_{YS}; these values are given for each test specimen in Table 2. Knowing σ_{AF}/σ_{YS} for a particular specimen, it was then possible to obtain theoretically predicted values of maximum stress from the stress analysis.

A final restriction on the analytical stress analysis developed is that it is valid only for cases where plastic deformation is confined to the immediate vicinity of the notch tip. The analytical analysis predicted that this condition would be satisfied provided the ratio between average applied stress and yield stress, σ_A/σ_{YS} was less than approximately 1.0; for values of σ_A/σ_{YS} greater than 1, yielding would be expected to progress from the notch root to the center of the specimen and gross plastic deformation would ensue. This predicted behavior from the analytical studies may be compared with the actual behavior of the test specimens. If the experimentally determined behavior of the specimens should compare favorably with predicted behavior, then the use of the experimental test results in the elastic-plastic stress analysis would seem to be justified. In room temperature tests, the average applied stress, σ_A, at which a marked increase in deformation would occur is predicted by the analysis to be approximately 30 ksi. From Fig. 16 it can be seen that the average applied stress corresponding to the beginning of extensive plastic deformation is approximately 32 ksi as indicated by both strain gage and extensometer measurements. Specimens tested at -100 F should undergo a marked increase in plastic deformation at an average applied stress of somewhere around 44 ksi. Figure 18 shows that the corresponding experimental stress is actually about 46 ksi. This is extremely good agreement since the experimental stress should be slightly higher than the predicted stress, at which unstable yielding is only beginning.

From Table 2 it can be seen that only for those specimens tested at -320 F, was yielding limited to the notch tip. For all of the other specimens tested at higher temperatures, the values of σ_{AF}/σ_{YS} were considerably larger than one, and in accordance with the definition of brittle fracture used in this report, fractures at test temperatures of -100 F and room temperature would be classified as ductile fractures since considerable plastic deforma-

TABLE 2. SUMMARY OF RESULTS.

Specimen* No.	Temperature (Deg.F)	σ_{af} (ksi)	σ_{af}/σ_{ys}	$(\sigma_y)_{max}$ (ksi)	$(\sigma_x)_{max}$ (ksi)	$(\sigma_z)_{max}$ (ksi)	τ_{max} (ksi)	τ_{max}/σ_{max}
H2-1	+ 78	**	--					
H4-2	+ 78	69.0	2.30					
H4-4	+ 78	**	--					
H6-2	+ 78	68.8	2.29					
H8-1	+ 78	68.6	2.29					
H8-4	+ 78	69.3	2.31					
H2-6	-100	78.4	1.78					
H4-1	-100	70.0	1.59					
H6-1	-100	63.7	1.45					
H6-4	-100	63.8	1.45					
H8-5	-100	72.1	1.64					
H8-6	-100	64.8	1.47					
H2-2	-320	62.1	0.54	232	113	104	64	0.28
H2-7	-320	53.2	0.47	217	97	94	61	0.28
H4-3	-320	58.9	0.52	227	109	101	63	0.28
H4-7	-320	82.0	0.72	269	151	126	72	0.27
H6-3	-320	67.8	0.59	243	123	110	67	0.27
H6-5	-320	78.1	0.68	263	143	122	71	0.27
H8-3	-320	79.1	0.69	264	145	123	71	0.27
H8-7	-320	73.6	0.64	254	134	116	69	0.27

* First number in Specimen Designation represents thickness in eighths of an inch; i.e., H6 is 6/8 or 3/4 in. thick.

** Shear Failures.

tion preceded fracture.

The results from the experimental work seems to substantiate the theoretical results and also give ample justification for applying the stress analysis to the experimental tests conducted at liquid nitrogen temperature.

Stress State at Fracture

The state of stress at the origin of fracture initiation is characterized by the values of the three principal stresses σ_Y, σ_X and σ_Z at that point. Fracture is assumed to initiate along the mid-thickness of a specimen at the elastic-plastic boundary on the minimum section of a notched specimen. At this point all three principal stresses attain their maximum values based on the analysis used.

The maximum axial and transverse stresses, $(\sigma_Y)_{MAX}$ and $(\sigma_X)_{MAX}$, along the minimum section of the specimen at the instant of fracture initiation can be determined by incorporating results from the experimental study into the elastic-plastic stress analysis developed in this report. The third principal stress, $(\sigma_Z)_{MAX}$, can then be determined from the appropriate plane strain relationships. The maximum axial tensile stress is most probably the critical stress governing fracture initiation, although whether or not this critical stress can be attained is likely a function of the other principal stresses as well as other variables such as temperature. For this reason, emphasis will be placed on the determination of the maximum axial tensile stress developed in the test specimen.

The procedure for calculating the maximum stress in the y-direction corresponding to a particular value of applied stress was discussed briefly on Page 2. An explanation of how the maximum axial stress at fracture in a typical test specimen can be found follows. For each specimen tested in the experimental phase of the program, the average applied stress at which fracture occurred was read directly from the testing apparatus, and the yield stress corresponding to the test temperature was determined from Fig. 12. The ratio of nominal fracture stress to yield stress σ_{AF}/σ_{YS}, could then be determined and these values are shown for all specimens in Table 2. If the

value of σ_{AF}/σ_{YS} was greater than 1, the fracture was classified as ductile according to the definitions of brittle and ductile used in this report, and the stress analysis was not applicable to these specimens. For specimens in which brittle fractures occurred, i.e., $\sigma_{AF}/\sigma_{YS} < 1$, the ratio of theoretical maximum axial stress to yield stress, $(\sigma_Y)_{MAX}/\sigma_{YS}$, corresponding to a particular value of σ_{AF}/σ_{YS}, was obtained from the relationship plotted in Fig. 9. The value of yield stress at each test temperature had previously been determined and hence the value of the maximum axial stress, $(\sigma_Y)_{MAX}$, could be calculated for every specimen that fractured in a brittle manner.

The values of $(\sigma_Y)_{MAX}$ for each specimen in which brittle fracture occurred are given in Table 2. The values of $(\sigma_Y)_{MAX}$, shown in Table 2, fell within a range from 217 ksi to about 270 ksi with an average value of 246 ksi, which may be considered to be within the limits of expected experimental and theoretical errors. The maximum variation from the average value was on the order of 10 per cent. At this stress, the region of yielding had progressed to an average depth of approximately 0.01 in. beneath the notch tip along the minimum section.

The extent of yielding as predicted by the analysis can be qualitatively verified by examining the strain gage records shown in Figs. 17 and 19. It will be noted that the response of the horizontal gages, located roughly 0.01 in. from the notch tip, shows a noticeable break at applied stresses of approximately 16 ksi and 24 ksi for the specimens tested at room temperature and -100 F respectively. In both cases, this is a ratio of σ_A/σ_{YS} equal to 0.55, which corresponds to a predicted position of the elastic-plastic interface approximately 0.01 in. from the notch tip.

The values of maximum stress in the x-direction (transverse), $(\sigma_X)_{MAX}$, were obtained in exactly the same manner in which $(\sigma_Y)_{MAX}$ was found. From the values of σ_{AF}/σ_{YS} available for each test specimen in the brittle range, corresponding values of the ratio of maximum transverse stress to yield stress, $(\sigma_X)_{MAX}/\sigma_{YS}$, were obtained from the relationship given in Fig. 10. $(\sigma_X)_{MAX}$ was then calculated and these values are given in Table 2. As can be seen from the table, the average value of $(\sigma_X)_{MAX}$ was approximately 127 ksi, but the range of stress values is somewhat wider than was observed for $(\sigma_Y)_{MAX}$, varying from a low value of 97 ksi to a high of about 151 ksi.

Since the conditions in specimens which exhibited brittle fractures were very close to plane strain conditions, the maximum stress, $(\sigma_Z)_{MAX}$, normal to the plane of the specimen could be easily calculated from the relationship

$$\sigma_Z = \upsilon(\sigma_X + \sigma_Y)$$

in which υ is Poisson's ratio, taken to be 0.3 in the elastic calculations. The average value of $(\sigma_Z)_{MAX}$ was found to be approximately 112 ksi and values of $(\sigma_Z)_{MAX}$ for each specimen are also presented in Table 2. The complete state of stress, defined by the three principal stresses at location and instant of fracture initiation, has thus been obtained.

Discussion of Results

The results obtained thus far from an application of the analytical stress analysis to experimental data suggest that a brittle fracture of the notched plate specimens of mild steel used in this investigation will occur only if a critical value of the maximum tensile stress is reached before yielding progresses across the minimum section of the specimen. For some specimens, yielding extended across the entire cross-section before the critical maximum tensile stress could be reached ($\sigma_{AF}/\sigma_{YS} > 1$) and the resulting fractures were ductile. This transition from brittle to ductile behavior occurs at a value corresponding approximately to $\sigma_A/\sigma_{YS} = 1$ which corresponds to a ratio of maximum tensile stress to yield stress, $(\sigma_Y)_{MAX}/\sigma_{YS}$ of about 2.88. The average value of the maximum stress that can be reached before initiation of fracture is 246 ksi and thus the yield stress corresponding to the brittle to ductile transition is approximately $\sigma_{YS} = \frac{246}{2.88}$ or $\sigma_{YS} =$ 85 ksi. For the material used in this investigation, a yield stress of 85 ksi corresponds to a test temperature of approximately -240 F. Thus for the particular specimen investigated, the transition from ductile to brittle behavior occurs at about -240 F. This, of course, is true only for static loading; for rapidly applied loads, the yield stress will be increased and consequently the brittle-ductile transition temperature will be higher.

From a knowledge of the three principal stresses at the origin of fracture initiation the maximum shear stress can be calculated from the expression

$$\tau_{MAX} = 1/2\ (\sigma_1 - \sigma_3)$$

where σ_1 and σ_3 refer to the maximum and minimum principal stresses respectively. For all specimens considered in this investigation, the maximum principal stress was always $(\sigma_Y)_{MAX}$ and the minimum principal stress, $(\sigma_Z)_{MAX}$. The average computed value of τ_{MAX} was about 67 ksi, and values of τ_{MAX} for each specimen are given in Table 2. The ratio of maximum shear stress to maximum tensile stress has been considered by most investigators to be a significant quantity in any fracture study, since τ_{MAX} and σ_{MAX} are the stress factors of greatest interest.[18]

As has been stated before, it is likely that mild steel will fracture brittlely when σ_{MAX} reaches a certain critical value; and plastic deformation is closely related to τ_{MAX}, becoming appreciable when τ_{MAX} reaches a critical value. Thus for a given set of test conditions, the ratio τ_{MAX}/σ_{MAX} will be an indicator of how the material will react to an applied load.

Values of the ratio τ_{MAX}/σ_{MAX} calculated for the test specimens are given in Table 2. Even though there was some slight variation in the calculated values of the stresses for the different specimens, it can be seen that the value of τ_{MAX}/σ_{MAX} was almost a constant for all tests, having a value of 0.27. It is possible that this ratio, when easily calculable, may be just as indicative of the final fracture mode of a specimen as would the maximum tensile stress. Below some critical ratio of τ_{MAX}/σ_{MAX} the resulting fracture would be brittle, while for values of τ_{MAX}/σ_{MAX} larger than the critical value, the fracture would be ductile. For the type of specimen used in this investigation at a test temperature of -320 F, the resulting value of τ_{MAX}/σ_{MAX} = 0.27 is obviously below the critical value.

The theoretical elastic stress concentration factor for the notch geometry used in this study was found to be approximately 9. For any material in which even limited plastic deformation occurs, the elastic stress concentration factor is admittedly an erroneous and unrealistic relationship between the maximum tensile stress in the vicinity of a notch and the average applied stress. However, for the specimens used in this study, an effective stress concentration factor, K_{EFF}, appropriate to the particular test conditions employed, can be determined as the ratio of maximum tensile stress at fracture to average applied stress, i.e., $K_{EFF} = \frac{(\sigma_Y)_{MAX}}{\sigma_{AF}}$. The average value of K_{EFF} calculated in this manner was approximately 3.6.

Comparison of Results with Previous Work

The approximate elastic-plastic stress analysis developed in this report has been shown to be valid for the types of specimens and the material used in this investigation. If this method of analysis is to yield results which can be regarded as a legitimate and reasonable approximation to the actual maximum stresses developed in mild steel, then results from this type of analysis should show reasonable agreement with results from other studies involving different specimen geometries and testing techniques. Although it is widely accepted that initiation of a brittle fracture is influenced predominantly by the maximum tensile stress reaching a critical level, relatively little work has been done to determine the value of such a critical stress, and thus limited data is available for comparison. The most significant studies in this area were conducted by Hendrickson, Wood and Clark[10] in an extensive series of tests on notched cylindrical specimens. By application of an elastic-plastic stress analysis to the experimental results, the investigation showed that brittle fractures were initiated in the mild steel employed when a critical tensile stress of approximately 210 ksi was attained. This value of critical stress was found to be independent of stress rate and temperature. From the investigation reported herein, the critical value of maximum tensile stress required for initiation of brittle fractures was found to be about 246 ksi.

Although of the same order of magnitude, the two values of critical tensile stress determined from the two investigations would be expected to show closer agreement since the material used in both cases was a mild steel of approximately the same chemical composition. One significant difference in the two investigations was the choice of a yield condition for use in the analytical analysis. If the Tresca

yield condition is used in analyzing the results of the investigation reported herein, rather than the Von Mises yield condition, it is found that the resulting critical tensile stress required for brittle fracture initiation is approximately 220 ksi, which compares very favorably with the value of 210 ksi previously predicted by Hendrickson and his associates.

Another source of comparison is possible by utilizing strain data obtained in the course of an investigation of brittle fracture propagation in wide steel plates conducted by investigators at the University of Illinois[19] as a part of Project SR-137. In Fig. 25 is presented values of peak dynamic strains measured during fracture propagation plotted as a function of distance from the fracture. If this data is extrapolated to obtain values of ϵ_X and ϵ_Y at the source of the fracture, the resulting strains are approximately ϵ_X = +1900 microin./in. and ϵ_Y = +7200 microin./in. Since these strains were measured on the surface of the test specimens, the corresponding stresses can be computed from the plane stress relationships:

$$\sigma_Y = \frac{E}{1-\upsilon^2} \left[\epsilon_Y + \upsilon \epsilon_X \right]$$

$$\sigma_X = \frac{E}{1-\upsilon^2} \left[\epsilon_X + \upsilon \epsilon_Y \right]$$

Calculated in this manner, the maximum tensile stress, $(\sigma_Y)_{MAX}$, at the tip of a propagating brittle fracture, is found to be approximately 256 ksi and the maximum stress in the transverse direction, $(\sigma_X)_{MAX}$, is 134 ksi. This is extremely good agreement with the theoretically predicted maximum values of 246 ksi and 127 ksi for $(\sigma_Y)_{MAX}$ and $(\sigma_X)_{MAX}$ respectively. Admittedly there is some scatter in the data, and the strain values obtained from extrapolation of the data in Fig. 25 is somewhat arbi-

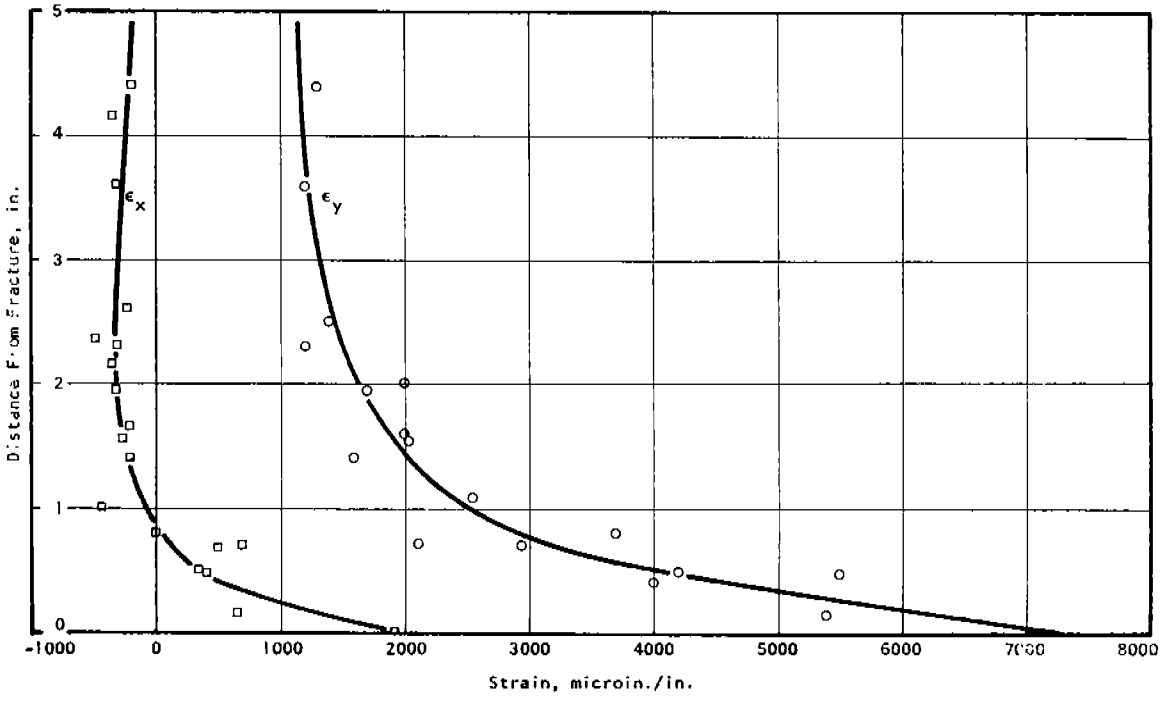

FIG. 25. PEAK STRAIN vs. DISTANCE FROM PROPAGATING FRACTURE IN WIDE PLATES (43).

trary. Nevertheless, any reasonable extrapolation of that data will give strains at the crack tip very close to those strains selected, and consequently the possible range of calculated maximum stresses will certainly be within the range of theoretical maximum stresses obtained from the experimental work conducted as a part of this investigation. This close comparison is felt to be especially significant since it is based on measured data rather than theoretical data of other investigators.

It is felt that the preceding comparisons give substantial justification to the validity and applicability of the stress analysis developed herein to other brittle-fracture studies in low-carbon steel.

SUMMARY AND CONCLUSIONS

Summary

The purpose of this investigation was to determine the general state of stress associated with brittle fracture initiation in mild steel, and in particular to determine the critical tensile stress necessary for fracture initiation. Also included as a part of this investigation was a study of the effects of certain parameters on fracture behavior. The results were obtained from both experimental tests of notched specimens and an analytical stress analysis.

In the experimental portion of the investigation, 2-in.-wide plate-type specimens of varying thicknesses, containing 1/2-in.-deep edge notches, were subjected to static tensile loading at different temperatures. Specimen thickness was varied from 1/4-in. to 1-in. and tests were conducted at temperatures of +78 F (room), -100 F and -320 F.

An approximate elastic-plastic stress analysis has been developed which provides a theoretical relationship between the average applied stress, and the principal stresses existing along the minimum section of a notched specimen. This analysis takes into account plastic deformation which is limited to the immediate vicinity of the notch tip. Application of this stress analysis to the experimental studies provided a theoretical prediction of the true state of stress at the instant and location of fracture initiation and also provided an indication of the position of the elastic-plastic boundary in the specimens.

Results obtained from this investigation have been compared with related work in fracture initiation studies to provide a basis for evaluating the particular stress analysis used and the reliability of the final results.

Conclusions

The significant results obtained from the investigation reported herein, and subsequent conclusions based on these results, may be summarized as follows:

(1) In the study of brittle fracture initiation in mild steel, the assumption of plane-strain conditions for plate thicknesses greater than 1/4-in.is apparently justified. This observation is based on the work of other investigators and also from results of the experimental work conducted as a part of this investigation.

(2) For the material and specimens employed in this investigation, a brittle fracture will initiate when the maximum tensile stress $(\sigma_y)_{MAX}$, reaches a "critical" value of approximately 246 ksi. This value of necessary stress for fracture initiation compares favorably with that determined from other analytical and experimental techniques.

At the instant of fracture initiation, the remaining two principal stresses, $(\sigma_x)_{MAX}$ and $(\sigma_z)_{MAX}$, were found to be approximately 127 ksi and 112 ksi respectively, and the maximum shear stress, τ_{MAX}, was calculated to be approximately 67 ksi.

(3) A brittle fracture has been defined in this study as a fracture preceded by only limited plastic deformation in the immediate vicinity of the notch root. Fractures occurring after yielding has extended across the entire cross-section of the specimen have been defined as ductile fractures. It was found that yielding would spread rapidly from the notch root to the axis of the specimen when the ratio of average applied stress to yield stress reached a critical value. This critical ratio of σ_A/σ_{YS} for the specimens tested, as predicted by the theoretical analysis and as determined from experimental measurements, is approximately equal to one. Thus a necessary condition for brittle fracture as defined herein is that the ratio of average applied stress to yield stress never reaches the critical value which would cause extensive plastic deformation.

(4) For the particular specimen geometry and material used in this study, the ductile to brittle transition will occur when the yield stress reaches a value of approximately 85 ksi. For static loading, this corresponds to a transition temperature of about -240 F.

(5) The position of the elastic-plastic boundary at fracture, as predicted by the theoretical analysis, was approximately 0.01 in. beneath the notch root along the minimum cross-section. This position of the yield zone was also qualitatively verified by results from the experimental work. The distance of the elastic-plastic boundary from the notch root, as determined by other investigators, was also found to be on the order of 0.01 in. in specimens of different geometry.

(6) Results from this investigation and the good agreement between these results and those obtained from other investigations indicate that the elastic-plastic stress analysis developed as a part of this study yields results which are consistent with similar results obtained from a more exact analysis. Thus the application and use of the analysis developed herein in studying brittle fracture in mild steel, in place of more complex and time-consuming methods of analysis, would seem to be justified.

By utilizing this approach, it should then be possible to predict the conditions under which brittle fracture will occur in mild steel specimens of other geometries.

(7) The effect of temperature on the average fracture stress of the notched specimens used in this investigation was found to be negligible. The significant effect of temperature, however, was on the yield stress and consequently on the fracture mode, resulting in the occurrence of brittle fractures at low temperatures.

(8) The average fracture stress apparently was independent of any thickness effect, at least within the range of thicknesses employed. This observation was to be expected, however, since plane strain conditions probably exist in the central regions of specimens for thicknesses greater than approximately 1/4-in.

ACKNOWLEDGEMENT

This technical report covers an adjunct study of an investigation on Low-Velocity Fracture sponsored by the Ship Structure Committee through the Bureau of Ships, U. S. Navy, Contract NObs 65790. The investigation was conducted in the Structural Research Laboratory of the University of Illinois. This report is based on a doctoral dissertation by F. W. Barton, submitted to the Graduate College, University of Illinois, 1962; Professor W. J. Hall served as thesis adviser. The authors wish to acknowledge the valuable assistance of Professor V. J. McDonald and Mr. F. F. Videon in connection with various phases of the study.

REFERENCES

1. Dieter, G. E., Jr., Mechanical Metallurgy. New York: McGraw-Hill, 1961.

2. Jenkins, D. R., Gascoigne, H. E., Wolf, L. W., and Clark, S. K., Effect of State of Stress on the Failure of Metals at Various Temperatures (WADD Technical Report 60-234). Wright-Patterson AFB, Ohio: Aeronautical Systems Div., July 1960.

3. Averbach, B. L., Felbeck, D. K., Hahn, G. T., and Thomas, D. A., eds., Fracture. New York: John Wiley & Sons, Inc., 1959.

4. Davis, H. E., Parker, E. R., and Boodberg, A., "A Study of the Transition from Shear to Cleavage Fracture in Mild Steel," Proceedings, ASTM, vol. 47 (1947).

5. Weiss, V., and Sessler, J. G., "Analysis of the Effects of Test Temperature on the Notch Strength of High-Strength Sheet Alloys," ASTM Preprint 80d, 1961.

6. Weiss, V., Sessler, J. G., Packman, P., and Sachs, G., The Effect of Several Geometrical Variables on the Notch Tensile Strength of 4340 Steel Sheet Heat Treated to Three Strength Levels (WADD Technical Report 60-310). Wright-Patterson AFB, Ohio: Aeronautical Systems Div., Sept. 1960.

7. Grinter, L. E., "Brittle Fractures Explained by Negative Residuals," Journal of the Engineering Mechanics Div., Proc., ASCE, vol. 87, no. EM2 (April 1961).

8. Yukawa, S., and McMullin, J. G., "Effects

of Specimen Size and Notch Acuity on the Brittle Fracture Strength of a Heat-Treated Steel," ASME Preprint 61 - Met-2, 1961.

9. Hendrickson, J. A., Wood, D. S., and Clark, D. S., A Preliminary Study of the Yielding of Notched Specimens under Rapidly Applied Tensile Loads (12th Technical Report under Office of Naval Research, Contract N6onr-24418, Proj. Designation NR031-285), California Institute of Technology, August 1955.

10. Hendrickson, J. A., Wood, D. S., and Clark, D. S., The Initiation of Brittle Fracture in Mild Steel (3rd Interim Technical Report under Office of Ordnance Research, OOR Proj. No. 1235, Contract No. DA-04-495-Ord-171), California Institute of Technology, April 1957.

11. Felbeck, D. K., and Orowan, E., "Experiments on Brittle Fracture of Steel Plates," The Welding Journal, 34:11, Research Supplement, p. 570-s (Nov. 1955).

12. Neuber, H., Theory of Notch Stresses: Principles for Exact Stress Calculation. Ann Arbor, Michigan: J. W. Edwards, 1946.

13. Allen, D. N. de G., and Southwell, Sir Richard, "Relaxation Methods Applied to Engineering Problems; XIV. Plastic Strain in Two-Dimensional Stress-Systems." Philosophic Transactions, Royal Society of London (Series A), vol. 242 (1949).

14. Southwell, R. V., Relaxation Methods in Theoretical Physics. Oxford, 1946.

15. Jacobs, J. A., "Relaxation Methods Applied to Problems of Plastic Flow; 1. Notched Bar under Tension," Philosophic Magazine, vol. 41 (1950).

16. Grubin, A. N., and Likhachev, U. I., "Analysis of Stresses Developing in the Stage of Large Plastic Deformations in Tension Tests of Cylindrical Specimens with Circular Notches," Zhurnal Tekhnicheskoy Fiziki (Russian), vol. 25, no. 3 (1955).

17. Sternberg, E., and Sadowsky, M. A., "Three-Dimensional Solution for the Stress Concentration around a Circular Hole in a Plate of Arbitrary Thickness," Journal of Applied Mechanics, March 1949.

18. Gensamer, M., Strength of Metals under Combined Stresses. Cleveland: American Society For Metals, 1940.

19. Rolfe, S. T., Lynam, T. M., and Hall, W. J., Studies of the Strain Distribution in Wide Plates during Brittle Fracture Propagation (Ship Structure Committee Report Serial No. SSC-118). Washington: National Academy of Sciences-National Research Council, December 30, 1959.

GPO 862-936

USCOMM-DC-51039